



ICELAND SCHOOL OF ENERGY
REYKJAVIK UNIVERSITY

**Review of H₂S Abatement in Geothermal
Plants and Laboratory Scale Design of
Tray Plate Distillation Tower**

Esteban José Rodríguez Pineda

Thesis of 60 ECTS credits

Master of Science in Sustainable Energy Engineering – ISE

December 2013



Review of H₂S Abatement Methods in Geothermal Plants and Laboratory Scale Design of Tray Plate Distillation Tower

Esteban José Rodríguez Pineda

Thesis of 60 ECTS credits submitted to the School of Science and Engineering
at Reykjavík University in partial fulfillment
of the requirements for the degree of
Master in Science in Sustainable Energy Engineering - ISE

December 2013

Supervisors:

Einar Jón Ásbjörnsson – Professor, Reykjavík University, Iceland.

William Scott Harvey – Professor Reykjavík University, Iceland

Examiner: Teitur Gunnarsson – Mannvit.

Abstract

Despite having significantly lower emissions in comparison to traditional fossil fuel plants, geothermal power plant emissions can still be substantial. In particular, dissolved non-condensable gases (NCG) such as CO_2 and H_2S within geothermal fluids have led to increased interest in developing methods for decreasing these emissions through abatement systems or even potentially using these gases to generate value for use in industrial processes.

A literature research was performed in order to review the most common abatement methods, their characteristics, advantages and limitations. The key variables identified during the literature research are the economics of the process, the ratio of ammonia-to-hydrogen sulfide in the geothermal brine and the condenser design. By using the criteria described in the work, some processes, or combination of processes are proposed. All of the methods suggested are considered effective, achieving over 90% removal of H_2S entering the geothermal field.

The methods that presented the most advantages included scrubbing with alkali, liquid redox methods, reinjection of NCG, Selectox, Dow-Spec RT-2 and BIOX.

Although many H_2S abatement methods are available and used in different geothermal plants across the world, few, if any, were economically feasible for Reykjavík Energy to operate in Iceland. However, it appears that using distillation as a method of abating H_2S emissions is potentially possible and perhaps economically beneficial in the particular context of Iceland. This process may lead to a system with relatively little equipment required but a relatively complex operation. Special care must be placed in material selection and prevention of gas hydrates forming inside the equipment.

Overall, it is recommended that this laboratory scale tower be built using modular design. This way, different materials can be tested at different operating conditions and the overall performance of the distillation tower can be evaluated.

Review of H₂S Abatement in Geothermal Plants and Laboratory Scale Design of Tray Plate Distillation Tower

Esteban José Rodríguez Pineda


60 ECTS thesis submitted to the School of Science and Engineering
at Reykjavík University in partial fulfillment
of the requirements for the degree of
Master of Science in Sustainable Energy Engineering – ISE

December 2013

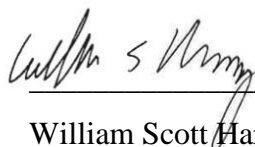
Student:

Esteban José Rodríguez Pineda

Supervisors:



Einar Jón Ásbjörnsson



William Scott Harvey

Examiner:

Teitur Gunnarsson

Acknowledgements.

Foremost, I would like to extend my sincere gratitude to my supervisors, Einar Jón Ásbjörnsson and William Scott Harvey for their support, patience, motivation, enthusiasm and constructive comments throughout the work on this thesis. They have provided me with much welcomed insights regarding the structure, content and narrative of many parts of this work.

I would also like to thank Magnús Arnarsson and Húni Sighvatsson for their help understanding the process at Hellisheiði and with the engineering considerations in the second part of my thesis. Without their help, several aspects of these thesis would have been much harder to work with.

In addition, I would like to thank the other students of this program, with whom I worked together over the course of these last 18 months and learned a lot from them.

Finalmente, quiero agradecer a mi familia y amigos en Guatemala y en Estados Unidos, porque sin su apoyo e insipración, la simple idea de estudiar en el exterior nunca habría podido materializarse.

Table of contents

Abstract.....	iii
Acknowledgements.....	v
Table of contents.....	vi
List of figures.....	viii
List of tables.....	viii
List of reactions.....	ix
1. Introduction.....	1
1.1. Main research motives.....	1
1.2. Thesis structure and approach	3
2. Review of H ₂ S abatement methods.....	4
2.1. Geothermal power emissions.....	4
2.1.1. Air Emissions	4
2.1.2. Regulations in Iceland.....	5
2.2. Non-condensable gases.....	6
2.2.1. Composition of non-condensable gases.	6
2.2.2. Impact of non-condensable gases on plant performance	7
2.3. Separation of NCGs from steam.....	8
2.3.1. Steam ejector vacuum systems.....	8
2.3.2. Liquid Ring Vacuum pumps	9
2.3.3. Dry Vacuum Pumps	9
2.3.4. Hybrid systems.....	10
2.3.5. Steam reboilers.....	10
2.4. Abatement of H ₂ S from alternatives.	11
2.4.1. From geothermal steam (Methods A)	12
2.4.2. Off-gas NCG removal equipment stream (Methods B)	14
2.4.3. Condensate water (Methods C).....	24
2.4.4. Hybrid System (Methods D)	25
3. Experience at Hellisheiði geothermal plant	26
3.1. Conception of the system.	27
3.2. Operation	27

4. Background on the process of Distillation.....	28
4.1. Properties of CO ₂ and H ₂ S	29
4.1.1. PVT behavior of pure substances.....	29
4.1.2. Carbon dioxide phase diagram.....	29
4.1.3. Hydrogen sulfide phase diagram.....	30
4.1.4. Binary Vapor-Liquid-Equilibrium	31
4.2. Distillation	33
4.2.1. General principles of distillation	33
4.2.2. Cryogenic distillation of gases.	34
4.2.3. Liquefaction	34
4.2.4. Liquefaction methods.....	35
4.3. The McCabe-Thiele design method.	37
4.3.1. Mass Balance	37
4.3.2. Feed and Operation and lines.	38
5. Clogging risks associated with gas hydrates.....	40
5.1. Gas hydrates	40
5.2. Clogging prevention techniques.	41
5.2.1. Thermal methods.....	41
5.2.2. Chemical methods.....	42
6. Results and discussion	45
6.1. Section with results regarding abatement methods.	45
6.2. Section with results regarding distillation	52
7. Conclusions.....	70
7.1. Conclusions for H ₂ S abatement methods.....	70
7.2. Conclusions for proposed distillation process	71
8. References.....	74
9. Appendices.....	82

List of figures

Figure 1: Classification of options for H ₂ S abatement [34].....	12
Figure 2: Carbon dioxide phase diagram	30
Figure 3: Vaporization curve of pure H ₂ S phase diagram.	31
Figure 4: VLE curve for CO ₂ -H ₂ S System at 40bar	32
Figure 5: VLE curve for CO ₂ -H ₂ S system at 20bar.....	34
Figure 6: Mass balance for distillation column.....	39
Figure 7: Drawing of number of ideal steps with McCabe-Thiele method.	41
Figure 8: Proposed H ₂ S abatement system selection decision tool.....	51
Figure 9: Process flow diagram of proposed system	60
Figure 10: Piping and Instrumentation Diagram of the proposed system	63
Figure 11: Correlation employed for calculation of Specific Heat at constant pressure of CO ₂ and H ₂ S, 4MPa.....	86
Figure 12: Correlation employed for the calculation of Specific Heat at constant volume of CO ₂ and H ₂ S, 4MPa.....	86
Figure 13: Correlation used for calculation of mixture boiling point 4MPa	87
Figure 14: Correlation used for calculation of heat capacity at constant pressure, 2MPa	87
Figure 15: Correlation used for calculation of heat capacity at constant volume, 2MPa	88
Figure 16: Correlation used for calculation of boiling point of mixture, 2MPa.....	88
Figure 17: McCabe Thiele Diagram of distillation process at 40bar	89
Figure 18: McCabe-Thiele Diagram of distillation process at 20bar	90
Figure 19: Kv values for perforated plates under flooding condtionst	91

List of tables

Table 1: Various environmental guidelines for H ₂ S air concentration emissions.....	6
Table 2: Non-condensable gas composition of geothermal steam in different fields [21].	7
Table 3: Methods for H ₂ S abatement.....	11
Table 4: Binary Vapor-Liquid Equilibrium Data for CO ₂ -H ₂ S System at 40bar [73]	32
Table 5: Binary Vapor-Liquid Equilibrium Data for CO ₂ -H ₂ S System at 20bar	33

Table 6: Criteria used for preliminary selection of H ₂ S abatement processes.	49
Table 7: Summary of recommended H ₂ S abatement methods.....	50
Table 8: Design basis for distillation process.	52
Table 9: Simplified mass balance for distillation process.	53
Table 10: Thermophysical properties calculated for the gas feed	56
Table 11: Tray spacing design possibilities for 4MPa conditions	57
Table 12: Tray spacing design possibilities for 2MPa conditions	58
Table 13: Distillation tower characteristics	60
Table 14: Distillation process mass balance	61
Table 15: Specifications for flow transmitter FT-1	62
Table 16: Specifications for automatic valves V-1, V-2, V-3 and V-6	64
Table 17: Specifications for level transmitter LT-1.....	64
Table 18: Specifications for pressure transmitter PT-1	65
Table 19: Specifications for automatic valves V-4 and V-5.....	66
Table 20: Specifications for Programmable Logic Controller.....	67
Table 21: Utilities required per kg of NCG	68
Table 22: Thermophysical properties of CO ₂ at 4MPa	82
Table 23: Thermophysical properties of H ₂ S at 4MPa	83
Table 24: Thermophysical properties of CO ₂ at 2MPa	84
Table 25: Thermophysical properties of H ₂ S at 2MPa	85

List of reactions.

Reaction 1: Initial reaction within the scrubber	13
Reaction 2: Formation of elemental sulfur	13
Reaction 3: Sodium sulfide formation	14
Reaction 4: Sodium hydrosulfide formation.....	14
Reaction 5: Sodium bisulfate formation	14
Reaction 6: Sodium sulfate formation	14
Reaction 7: Stretford process reaction	15
Reaction 8: Sulfur precipitation in SulFerox reaction	16
Reaction 9: Iron regeneration in SulFerox process.....	16
Reaction 10: Simplified Hiperion chemical reaction.....	17

Reaction 11: Xertic Process reaction.	20
Reaction 12: Absorption reaction in Fe-Cl hybrid method.....	21
Reaction 13: Electrolysis during Fe-Cl hybrid method.	21
Reaction 14: Absorption reaction in THIOPAQ process.....	22
Reaction 15: Oxidation reaction in THIOPAQ method.....	22
Reaction 16: Acidic environment reaction	24
Reaction 17: Caustic environment reaction.	24

1. Introduction

1.1. Main research motives

Demand for energy and associated services are necessary to meet social and economic development and improve human welfare and health. Most aspects of the modern lifestyle have some connection to energy, whether it involves traveling to work, for vacation, cooking, cleaning, communication, space comfort, etc. Since approximately 1850, global use of fossil fuels has increased, leading to a rapid growth in carbon dioxide (CO₂) emissions [1].

The greenhouse gas emissions resulting from this type of fuel-burning have also increased dramatically, and recent data confirm that the consumption of fossil fuels accounts for the majority of global anthropogenic emissions. Carbon dioxide concentrations have increased to over 390ppm, some 39% above preindustrial levels. The IPCC Fourth Assessment Report concluded that “most of the observed increase in global average temperature since the mid-20th century is very likely due to the observed increase in anthropogenic greenhouse gas concentrations [1].

There is no question that energy must continue to be harnessed in order to improve human welfare and health, as it has been done up until now. The question is whether or not there exist energy sources that can reduce the current dependence on fossil fuels and reduce the greenhouse gas emissions that result from their use. And, if these technologies can serve as a substitute, if they can be managed and used in such a way as to minimize their own gas emissions, if any.

There are multiple options for substituting fossil fuel technology and reduce greenhouse gas emissions from the worldwide energy system, while satisfying the global demand for energy. Some of these options include energy conservation, energy efficiency, hydropower, geothermal, solar, wind or nuclear energy. Geothermal energy has been extensively used in Iceland. Geothermal energy has increased since the seventies as a result of increased use for house-heating and over the last decade due to increased use for the generation of electricity [2].

It is estimated that in 2010 there was approximately 10,715 MW of installed geothermal power in the world, which represents an increase of 20% over 2005 levels [3]. Geothermal energy presents a series of advantages over other energy sources.

Geothermal energy is a widely available resource, which is economically viable in many of the volcanic regions of the world. Also, it requires minimal land and water usage compared to other generation types [4]. One of the most important technical advantages of geothermal energy is a capacity factor similar to nuclear or other traditional fossil fuels, meaning it can supply base load power in ways other intermittent renewables sources, such as solar or wind, cannot.

However, one of these main advantages poses a significant problem for the continued development of geothermal resources. Despite having significantly lower emissions in comparison to traditional fossil fuel plants, geothermal power plant emissions can still be substantial. In particular, dissolved non-condensable gases such as CO₂, H₂S within geothermal fluids have led to increased interest in developing methods for decreasing these emissions through abatement systems or even potentially using these gases to generate value for use in industrial processes.

One of these gas emissions, H₂S, has become a point of discussion recently, since increasing development of geothermal resources near Reykjavík has resulted in increasing H₂S exposure on residents of the Reykjavík Capital Region, as well as other surrounding areas [5]. A 2010 report on air pollution in Iceland by the European Environmental Agency, found that there is some evidence of corrosion on electronic equipment due to H₂S emissions [6]. This, in combination with lack of research on chronic, low level of H₂S exposure [7], has resulted in significant public concern as to the unforeseen side effects of H₂S pollution. In response to this, the Department of Environment of Iceland began taking measurements of H₂S in the vicinity of Reykjavík in 2006 with the objective of monitoring the impact of geothermal power plants on the air quality in the capital area. Similarly, this resulted in the Minister of Environment issuing Regulation 514/2010, discussed below, regulating the maximum concentration of H₂S in the atmosphere [8].

With all of this in mind, this thesis explores some of the most widely used H₂S abatement methods in the industry in an attempt to bring together the experience accumulated over the years in this topic. At the same time, it attempts to serve as a decision tool for choosing abatement methods among geothermal fields of different non-condensable gases characteristics.

The second part of this thesis explores one subset of these many processes: the distillation of both CO_2 and H_2S as a different method of abatement. It provides the design of a small scale distillation system, with a modular-form design with the intent of providing a framework for implementing a large scale pilot plant operation of this proposed abatement method.

1.2. Thesis structure and approach

The first chapter of this thesis serves as the introduction into the motivation behind this project, as well as a description of the project itself.

Chapter 2, Review of H_2S abatement methods, serves as the literature review for the H_2S abatement section of the thesis. This section presents an overview of the geothermal power gaseous emissions and puts in context the regulations in effect in Iceland. At the same time, it discusses how these non-condensable gases are emitted, why they are present in the geothermal brine and what is the technical reason behind their emission, including some techniques used for the separation of the NCG's from the steam. This chapter ends by discussing some of the abatement alternatives developed throughout time, their advantages and disadvantages, including commercial experience of the most widely used methods.

Chapter 3, Experience at Hellisheiði geothermal plant, presents a brief overview of the work Reykjavík Energy has done at Hellisheiði, particularly how the abatement system was conceived, its operation and some of the problems they encountered.

Chapter 4, Background on the process of Distillation, serves as the literature review for the distillation section of the thesis. This section discusses the important thermodynamic properties of CO_2 and H_2S to the process of distillation, as well as a brief overview on the general principles of distillation, gas distillation, liquefaction and liquefaction methods.

Chapter 5, Clogging risks associated with gas hydrates, presents a brief overview of the clogging risks associated with attempting to distill CO_2 and H_2S along with a brief overview of the prevention techniques developed by the oil and gas industry.

Chapter 6, Results and discussion, presents the main results of the thesis, along with an examination of the findings, with the conclusions presented in Chapter 7.

Chapter 8, References, presents the literature reviewed along the making of the thesis. Finally, Chapter 9, Appendices, presents the information used for estimating the properties required in the design phase of this work.

2. Review of H₂S abatement methods

2.1. Geothermal power emissions

Geothermal energy is an environmentally friendly, renewable and sustainable source of electricity. Some types of geothermal power plants release gases into the atmosphere during energy conversion due to the presence of naturally occurring dissolved gases contained in the geothermal brine. Since this form of energy conversion does not involve direct combustion of any kind, the emitted gases are limited to those carried in the geofluid in dissolved form.

Compared with other forms of energy production, geothermal power is environmentally nonthreatening. According to [9], a typical geothermal power plant using hot water and steam to generate electricity emits about 1% of the sulfur dioxide (SO₂), less than 1% of the nitrous oxides (NO_x) and 5% of the carbon dioxide (CO₂) emitted by a coal-fired plant of equal size. For example, the combustion of coal emits about 900 kg of CO₂ per MWh. In contrast, geothermal power plants release about 120 kg per MWh [9], or as low as 50 kg per MWh [10], depending on the characteristics of the geothermal brine. Other gases, such as methane, hydrogen or ammonia, can also be found, usually in very low concentrations [10]. Binary geothermal plants have virtually insignificant GHG emissions compared to fossil fuels unless it operates by flashing geothermal brine, in which case the gas emissions would be equal to a typical flash plant. If that is not the case, the gas emissions of binary plants can be limited to working fluid leakage, which is typically a very small percentage of the total inventory per year (<1%) [11].

2.1.1. Air Emissions

2.1.1.1. Nitrogen Oxides

Nitrogen oxides are often colorless and odorless, and form during high temperature combustion processes from the oxidation of nitrogen present in the air, or liberated from the fuel. Motorized vehicles and fossil fuel power plants are the two major sources of these pollutants. Because geothermal plants do not burn fossil fuel, they emit very low levels of nitrogen oxides. As a matter of fact, in most cases, they emit no nitrogen oxides at all [12].

2.1.1.2. Hydrogen Sulfide

Hydrogen sulfide is a colorless gas that can have adverse health effects. Even at small concentrations, it is often regarded as an annoyance due to its distinctive “rotten egg” smell. Natural sources of this gas include volcano gases, natural gas, geothermal hot springs and fumaroles [12]. A 1979 study found H₂S to be the single most significant health concern related to geothermal energy development due to the risk of it causing several physiological response, such conjunctival irritation (10-20ppm), irritation of the respiratory tract (50-100ppm), olfactory paralysis (150-250ppm), pulmonary edema (320-530ppm), up to respiratory paralysis leading to death or neural paralysis (530-2000ppm) [13] [14]. Since 1976, H₂S emissions from geothermal sources have declined from 863kg/hr to 90kg/hr or less, although geothermal power production has increased from 500MW to over 2000MW. This translates as a decrease from approximately 1.92 kg/MWh to an average of about 0.085 kg/MWh [12].

2.1.1.3. Sulfur Dioxide

Sulfur dioxide (SO₂) is not directly emitted by geothermal power plants. However, the hydrogen sulfide they emit can react in the upper atmosphere to produce SO₂. It is estimated that flash geothermal power plants emit, albeit indirectly, 0.16kg/MWh of SO₂, compared to 4.72kg/MWh, in coal-burning power plants, and 5.45 kg/MWh in oil-fired plants respectively [12].

2.1.1.4. Carbon Dioxide

The main greenhouse gas emission from geothermal power plants is CO₂. One study concluded that geothermal power plants emit between 4 and 740 gCO₂/kWh, depending on design and composition of the geothermal fluid in the geothermal reservoir, with a weighed average of 112 gCO₂/kWh [15]. Other forms of energy conversion have an estimated CO₂ emission of approximately 930g/kWh, 1170 g/kWh and 1689 g/kWh for natural gas, oil and coal, respectively [15].

2.1.2. Regulations in Iceland

In response to the new monitoring data the Minister of Environment has issued Regulation 514/2010 regulating the maximum concentration of H₂S in the atmosphere. This became effective in July 2010. This regulation limits H₂S to 50

$\mu\text{g}/\text{m}^3$ average in a 24 hour floating period. The regulation aims to prevent or reduce potential harmful effects on human health, sensitive equipment and the environment. Entities are allowed to exceed this limit by 5 times a year until July 2014 but after this point the maximum concentration cannot be exceeded without penalty of law. Moreover the regulations make strides to ensure sufficient measurement of H_2S concentration and sets up a system for providing relevant information to the public [8]. This is a 66% reduction from the World Health Organization's (WHO) regional guidelines for Europe of $150 \mu\text{g}/\text{m}^3$ [14].

These new laws place high demands on the Icelandic geothermal industry to reduce current H_2S emissions levels which currently exceed the new limits multiple times per year [5]. In order to meet these strict regulations, commercially viable methods must be implemented to reduce the amount of H_2S vented to the atmosphere.

For comparison purposes, Table 1 provides other guidelines enforced in the United States and New Zealand.

2.2. Non-condensable gases

Non-condensable gases (NCGs) are naturally occurring in geothermal fluids. The relative proportions and quantities of NCGs vary from field to field, and sometimes from well to well within the same geothermal field. In geothermal power plants, NCGs accumulate in the condenser, decreasing heat transfer and raising the turbine backpressure, thereby lowering turbine performance. [19]

2.2.1. Composition of non-condensable gases.

The most common non-condensable gases in geothermal fluids are CO_2 , H_2S , H_2 , Ar, NH_3 , and CH_4 . The concentration of NCG's in the geothermal steam depends on

Table 1: Various environmental guidelines for H_2S air concentration emissions

Country/agency	Limit	Averaging period
New Zealand [16]	$7 \mu\text{g}/\text{m}^3$	1 hour
USEPA California [17]	$43 \mu\text{g}/\text{m}^3$	1 hour
Bay Area [18]	2.5 kg/hr	-
Iceland [8]	$50 \mu\text{g}/\text{m}^3$	1 hour
World Health Organization guidelines for Europe [14]	$150 \mu\text{g}/\text{m}^3$	1 hour

the characteristics of the reservoir. Typical concentrations of NCG's can vary from less than 0.2% to over 25% wt% of steam [20], but, as stated above, the exact quantity varies from field to field. Table 2 gives an overview of different geothermal fields around the world and their gas compositions.

Table 2: Non-condensable gas composition of geothermal steam in different fields [21].

Geothermal Field	Gas Composition (%weight)				
	CO ₂	H ₂ S	N ₂	H ₂	CH ₄
Olkaria (Kenya)	80.67	9.28	1.72	7.68	0.65
Wairakei (New Zealand)	88.67	10.02	0.80	0.24	0.25
Ngawha (New Zealand)	95.88	1.01	0.30	0.28	2.52
Zunil (Guatemala)	96.24	2.51	0.80	0.43	0.02
Miravalles (Costa Rica)	98.24	0.60	0.80	0.33	0.03
Svartsengi (Iceland)	92.54	2.32	4.98	0.10	0.06
Hveragerdi (Iceland)	75.32	7.11	15.80	1.62	0.15
Krafla (Iceland)	86.16	9.29	2.62	1.87	0.06
Hellisheiði (Iceland) [22]	72.55	23.53	1.96	N/A	N/A

2.2.2. Impact of non-condensable gases on plant performance

The presence of CO₂, or any other NCG in geothermal steam results in a significant decrease in the net power output. As Khalifa and Michealides, [23] points out, the work of the turbine decreases by almost 0.5% for each additional 1% increase in the mass fraction of CO₂. When the effects of the non-condensable gases are taken into account in the condenser stage, the net work output of a geothermal plant drops even more. The presence of 10% CO₂ in the geothermal steam can result in as much as 25% decrease in the net work output compared to a clean steam system. Therefore, the reduction in turbine power and the parasitic load of a NCG removal system must be balanced in order to optimize the power output of the plant.

2.3. Separation of NCGs from steam

The following sub-sections discuss the technologies and methods currently available to separate the NCGs from geothermal process fluids. The efficiencies of the separation processes are not discussed as they vary greatly with the composition of the geothermal resource. Note that removing the NCG stream from the condenser is an intrinsic part of the power generation process. Separation of the remaining NCG content dissolved in the condensate, which is controlled by NCG solubility in water at condensing pressure, is known as “secondary abatement” and is also discussed in this section.

2.3.1. Steam ejector vacuum systems

Steam ejectors are used broadly in conventional geothermal power plants for the extraction of non-condensable gases from the condenser. These systems offer a simple and reliable way of producing a vacuum with a relatively low installation cost [24]. They operate based on the Venturi principle with two inlet nozzles and a discharge nozzle. In one inlet, a motive fluid (usually steam) is expanded through a nozzle where it gains speed, forming a vacuum chamber inside. At the same time, on another inlet, the steam, which needs to be cleaned, enters. After leaving the nozzle at supersonic speed, the steam passes through the suction chamber and enters the converging diffuser as gas and associated water vapor [20]. They can also be installed in parallel when the load is variable or when maintenance shutdowns are required. If installed in series, an even lower vacuum pressure can be achieved [25].

Ejector systems can be classified as single-stage or multistage. Multistage ejector systems can be further classified as condensing or noncondensing. The single-stage ejector, which is the simplest type, can be used for pressures as low as 0.1 bar-a. Multistage non-condensing ejectors are used to produce suction pressures lower than this, can be more efficient than single stage compression, and hence are more common. Ejectors have a lower installed cost than pumps, so they are more frequently used in projects where low initial cost is more important than long-term costs. They also have no moving parts, facilitating maintenance and keeping operation fairly constant, are quiet, are easy to install, and handle corrosive steam mixtures [25] [26]. When installing multistage ejectors in series, each needs to discharge into an intercondenser. The function of the intercondenser is to condense the first stage

motive fluid and to remove the part of water vapor that initially saturated the non-condensable gas. This way, the second ejector handles only a minimal amount of water vapor and mainly the non-condensable gases in the steam [11]. This minimizes the required motive fluid for the overall process and ensures that a minimum of water vapor is discharged with the non-condensable gas [20]

2.3.2. Liquid Ring Vacuum pumps

A liquid ring vacuum pump is the second most often used vacuum system in geothermal power stations. This equipment has an impeller with blades attached but offset from the center of the cylindrical body. The impeller is between two plates, which have holes cut into them, called ports. The body of the pump is partially filled with a liquid sealant in a way that, when the pump is not operating, the bottom blades are immersed in the liquid while the top blades are not. Once it begins to rotate, the impeller forces the liquid to the outer edges by centrifugal force, forming a ring of liquid. When this happens, a large pocket is formed in the inlet side of the casing. The void space without the liquid is called an impeller cell. While the blade rotates, the impeller cell decreases in size and, air, gases or vapor flow through the inlet port and is exhausted to the atmosphere due to the compression of the liquid seal [26]. This relatively simple design minimizes noise and vibration as well as maintenance time [27].

2.3.3. Dry Vacuum Pumps

A dry pump is commonly used in larger-size pump applications. Three different types exist: rotary-claw, rotary-lobe and rotary-screw pumps. The rotary-claw type allows for a greater compression ratio to be taken across the rotors at higher pressures. A minimum of three stages in series is required to achieve pressures comparable to those in a liquid-ring pump. A rotary lobe pump is used as a booster, operating in series usually with a liquid seal pump. A rotary-screw pump uses two synchronized helical rotors in parallel. These types of pumps operate at high rotational speeds, increasing net pumping capacity. Because they do not produce condensate, they can be fabricated with inexpensive, standard cast iron. However, they are difficult to repair and may require cooling of the bearings and seals [27].

2.3.4. Hybrid systems

Hybrid systems consist on any combination of the equipment described above. For example, a combination of steam jet ejectors and centrifugal compressors are mentioned in [28] and [29] while [30], [31] and [32] report on plants equipped with combined steam jet ejectors and liquid ring vacuum pumps.

2.3.5. Steam reboilers

This option to removed NCGs consists of condensing and reboiling of the geothermal steam. Through this mechanism, it is expected that the bulk of non-condensable gases escape the steam with the condensation along with a small quantity of uncondensed steam, which acts as a carrier [33] [34]. The vent gases can be further treated downstream to control H₂S atmospheric emissions. This process can produce clean steam but with lower mass flow rate and enthalpy content in comparison to non-treated steam.

During 1979 and 1980, a feasibility study of this concept was carried out at The Geysers. During more than 1000 hours of accumulated test time, the average H₂S removal efficiency obtained was 94% and the heat transfer coefficient was high enough to make the cost of the heat exchanger competitive against other H₂S abatement system costs [35].

During 1984 and 1985, another test unit was built in Cerro Prieto, México, to evaluate the process in a liquid-dominated geothermal resource. It was reported that the process was capable of removing 94% by weight of non-condensable gases from geothermal steam [35].

In 1999, a test program was developed at the Kizildere power plant, Turkey, to demonstrate the process' general performance and show its applicability to the existing geothermal conditions. The test consisted of approximately 260 hours of run time over a 3-month period of time. In it, a packed bed direct contact reboiler process was built, which consisted in a direct contact condenser and a flash tank vessel. Steam was fed under the packed bed of the condenser and flows upward, where most of it is condensed in the packed bed. The non-condensable gases, along with a small amount of steam, are vented through a vent stream from the top of the condenser. The condensate flows to the flash tank through a valve. Here, part of the condensate is

flashed to a lower pressure and the remaining condensate is collected and sent to the top of the condenser as cooling water [35]

It was found that the average CO₂ removal efficiency was approximately 76.3±22.6% for a wide range of reboiler parameters, varying according to the vent rate. The main problems encountered during the test were related to control of the operation because the unit was controlled manually. Also, it was observed that the lack of mist eliminator in the condenser caused the drift of cooling water through the vent stream, causing a drop in the CO₂ removal efficiency [35].

2.4. Abatement of H₂S from alternatives.

Stephens, et al. [36] describes two main approaches for removing H₂S: before the steam flow reaches the turbine (upstream) and after the turbine (downstream). Sanopoulos and Karabelas [34] further classify the different methods according to the type of flow the method has to deal with for abating H₂S. Table 3 below describes these groups and Figure 1 illustrates the location for these methods in the power plant diagram [21] [34].

Table 3: Methods for H₂S abatement.

Method	Location	Type of flow
Method A	Upstream	Geothermal steam
Method B	Downstream	Off-gas ejector
Method C	Downstream	Condensate water
Method D	Downstream	Combination of flows

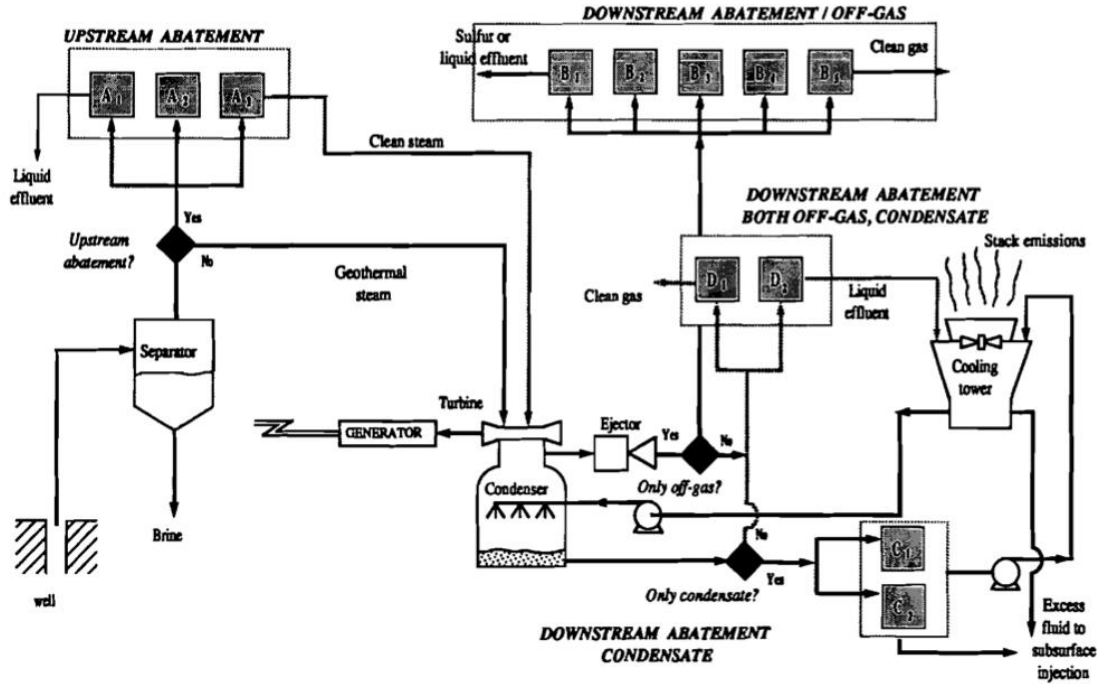


Figure 1: Classification of options for H₂S abatement [34].

2.4.1. From geothermal steam (Methods A)

Type A Methods are the only methods that eliminate H₂S upstream and, as such, are concerned with the totality of the steam entering the turbine. The main advantages of removing the H₂S at this point in the process is the possibility of eliminating H₂S emissions during steam stacking. This arises when a problem is detected in the power plant and the supply to the steam turbine has to be cut off. To prevent a possible burst of the steam pipeline due to a buildup of pressure, the relief valves in place open and the steam is vented directly into the atmosphere. Evidently, all methods concerning abatement of H₂S downstream of the turbine prove unsuccessful in the event that emergency conditions require shutdown of the turbine and a bleed of the geothermal steam.

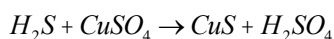
At the same time, these methods protect the turbine components from corrosion and scaling due to contact with the non-condensable gases. With this reduction of non-condensable gases entering the condenser, there is a backpressure reduction during normal operation, which leads to improved power production. However, as pointed out by [34], there is an inherent loss of steam and its associated enthalpy from these treatments.

This section will present a brief overview of the following processes:

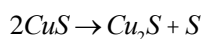
- Copper sulfate or EIC process.
- Scrubbing with an alkali solution.
- Steam reboiler (discussed previously)

2.4.1.1. *Copper sulfate or EIC process*

According to [36], in this process, the steam is contacted in a scrubber with a solution of copper sulfate (CuSO_4). The initial chemical reaction is shown in Reaction 1. The copper sulfide can later produce elemental sulfur, as shown in Reaction 2.



Reaction 1: Initial reaction within the scrubber



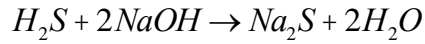
Reaction 2: Formation of elemental sulfur

The copper sulfate can be regenerated through two means. One is to combust the copper sulfide to produce copper sulfate. However, this process can also produce sulfur dioxide, which would need to be scrubbed or treated accordingly. The other way of regenerating the copper sulfate is to make a slurry of copper sulfide in sulfuric acid solution and treat it with oxygen under high pressure and temperature. The main byproduct formed by these series of reactions is elemental sulfur. This byproduct would require being disposed either by chemically treating it for the production of other useful sulfur-based chemicals or sold directly as fertilizer.

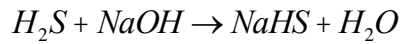
More recently, ter Maat, Hogendoorn and Versteeg, [37] have extended this procedure by investigating the removal of H_2S from gas streams using FeSO_4 and ZnSO_4 . Under laboratory scale conditions, they showed that iron carbonates can precipitate when CO_2 is in the gas, which makes FeSO_4 an unlikely suitable absorbent. On the other hand, their experimental results show that, when using ZnSO_4 , the formation of zinc carbonate can be avoided if the pH of the solution is regulated between 2 and 2.85. Finally, on a pilot plant scale, they showed that the removal of H_2S from biogas takes places very efficiently when using a co-current operated packed bed reactor using fresh and regenerated CuSO_4 . They found no problems with respect to plugging in the packing by the precipitate although they raise the issue that foaming is likely to occur for long operation times.

2.4.1.2. Scrubbing with Alkali

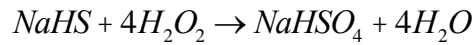
This process consists of scrubbing the geothermal steam or non-condensable gases with alkali, usually a solution of NaOH. As pointed out by [38], abatement of H₂S in steam occurs by reaction with NaOH to produce NaHS and water, as shown below in Reaction 3, Reaction 4, Reaction 5 and Reaction 6.



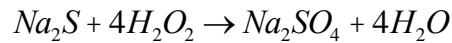
Reaction 3: Sodium sulfide formation



Reaction 4: Sodium hydrosulfide formation



Reaction 5: Sodium bisulfate formation



Reaction 6: Sodium sulfate formation

It is essential to use hydrogen peroxide (H₂O₂) as this prevents redistribution of sulfide ions if the pH changes occur later on.

If the excess NaHS can be recovered with the appropriate purity, it could be sold abroad. Sodium hydrogen sulfide is a solid flake that can be used in water treatment facilities, the paper manufacturing process and in leather processing. Given its yellowish color, it can also be used in the manufacture of dyes and artificial coloring. In mining, it can be used as a flotation agent to separate impurities.

2.4.2. Off-gas NCG removal equipment stream (Methods B)

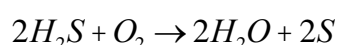
Methods B are concerned with the stream of gas exiting the condenser through a non-condensable gas removal system. These processes are usually chemical processes that produce elemental sulfur from the H₂S content. Depending on how each particular process operates, some abatement systems may require a surface condenser, but some may still be used with a direct contact condenser.

This section will describe the following abatement methods:

- Liquid redox methods
 - Stretford, Unisulf, SulFerox, Hiperion, LO-CAT and LO-CAT II
- AMIS
- Non-condensable gas injection systems.
- Peabody-Xertic process
- The Fe-Cl hybrid method
- Selectox
- Biological/THIOPAQ methods
- Burner-scrubber process.

2.4.2.1. Stretford

The Stretford process is a Vanadium-based process, which converts H₂S to sulfur by catalytic air oxidation. A solution of sodium carbonate, sodium metavanadate and anthraquinone disulfonic acid (ADA) is used as scrubbing medium in a counter-current scrubber. The sulfur is recovered as a floating product in a skimming tank. Sulfur solids are separated from the slurry in the tank using techniques such as filter press, centrifuge, etc. [39] The overall sulfur recovery process is governed by the following reaction, while the ADA acts as a replenisher of the vanadium [38]:



Reaction 7: Stretford process reaction

The Stretford process has proven to be very successful at The Geysers geothermal field for the past 30 years, where 15 Stretford units were installed during 1979-1989 and 13 are currently operating [40]. In general, this process will eliminate more than 99% of the H₂S in the gas processed [38] and it reaches 99.99% removal efficiency at The Geysers [40].

As reported by Farison, [40], the Stretford units at The Geysers have operated very well, with minimum downtime and little problems regarding vanadium and Stretford solution disposal. Normal process operation at The Geysers include a continuous monitoring of the tailgas to provide an early warning of out-of-limit conditions so corrective action can be taken, and an automated, liquid feeding

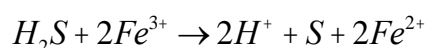
chemical system, rather than manual, solid feeding. This results in consistent chemical solutions and fewer chances of operator error.

2.4.2.2. *Unisulf*

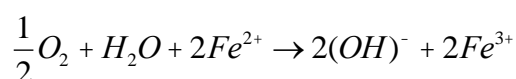
The Unisulf process is a vanadium-base process that uses a solution for absorbing H₂S from gas streams and oxidizing to elemental sulfur. Marketed by Unocal, the process' chemistry has been modified to eliminate by-product salt formation, such as thiosulfate and sulfate. This process offers the same high H₂S absorption efficiency as a Stretford solution with the added benefit of a lack of solid deposition, which minimizes the solution disposal problems associated with Stretford-operating plants [41] [42]

2.4.2.3. *SulFerox*

This process involves the usage of chelating iron compounds in a concentrated solution to oxidize the H₂S to elemental sulfur. The gas containing H₂S reacts with the dissolved iron in a contactor to form elemental sulfur. The treated gas flows to a separator where the gas is vented to the atmosphere and the solution is sent to a regenerator where the chelated iron is renewed. Sulfur settles in the regenerator and is taken from the bottom to filtration where sulfur cake is recovered. Reaction 8 and Reaction 9 show the two reactions involved in this process [43].



Reaction 8: Sulfur precipitation in SulFerox reaction



Reaction 9: Iron regeneration in SulFerox process

A technical report issued by the World Environment Center released in 1994, [44], mentions the use of this method in the Bureau of Land Management BLM-East and BLM-West plants at the Coso field. These plants, at the time, were producing 7.10 and 8.8 long tons per day of sulfur, respectively. At these plants, the demisters installed in the vent stacks had to be removed because they quickly fouled with sulfur after start-up. Similarly, plugging due to fouling was frequently observed in the heat exchanger tubes, water lines and pipe contractors. Regarding pump operation,

mechanical seal failures did occur during operation because of the significant amount of solid sulfur contained in the liquid [44].

2.4.2.4. *Hiperion*

This process uses a chelated iron catalyst combined with naphthaquinone to remove H₂S from hydrocarbons. This system is an improvement of the Takahax process used in Japan, with faster reaction dynamics, which reduces the equipment size required. The gas/liquid contactors use beds of a patented material that is resistant to pH changes and to plugging. The operating experience of this process is limited [45] [41].

The only literature found on the industrial application of this process, as well as the Takahax process, was in petroleum refineries. The first commercial use in the United States was in an asphalt refinery, where its purpose was to remove the H₂S from heavy gas oil. Similarly, a Hiperion system was developed to remove H₂S from an anaerobic digester used in municipal wastewater treatment plants [46].

The basic reaction in this process is shown below in Reaction 10. A more detailed chemical reaction involves a naphthaquinone chelate reduction to hydroquinone and to form elemental sulfur. This reaction is dependent on pH. Below pH=7, an undissociated H₂S is the predominant species and above pH=9, the S⁻² is predominant [46]



Reaction 10: Simplified Hiperion chemical reaction.

2.4.2.5. *LO-CAT*

This abatement method uses an extremely dilute solution of iron chelates. The gas containing the H₂S reacts with the iron solution in an absorber to form elemental sulfur, which is removed through centrifugation. The reactions involved in this process are the same as in the SulFerox process [43].

Merichem Chemicals and Refinery Services LLC published a bulletin in 2009 [47] pointing out the success of the LO-CAT system in the Coso geothermal field, California. There, it is mentioned that three LO-CAT systems were installed to handle the gas streams from 6 geothermal plants. Over the 15 years of operation, up to the publishing of the bulletin, the Lo-Cat units have consistently posted efficiencies above 99.99% in terms of H₂S removal. Their system uses solutions of KHCO₃ and

K₂CO₄ as buffers, which results in the unit's performance staying fairly constant, with changes never occurring immediately, but rather over long periods of time.

2.4.2.6. *LO-CAT II*

This process is the most widely used liquid redox system and is considered to be the best available control technology for geothermal power plants [12]. This process employs a ferric catalyst to oxidize the H₂S, producing elemental sulfur and water. All reactions in this process take place in a liquid phase. This system is expensive to install but is very inexpensive to operate, with costs usually ranging from \$200 to \$250 per tonne of H₂S. The LO-CAT II process can achieve up to 99% removal efficiency of H₂S [48], like the Stretford process described above.

Chelated iron and vanadium processes share operating problems, such as the foaming of the solution, clogging of pipes and vessels as well as some chemical and catalysts losses [39].

According to [44], chemical losses and plugging in the water lines have not been a problem in the Navy I and Navy II units of the Coso geothermal field.

2.4.2.7. *AMIS*

The Italian electric utility company, ENEL SpA, developed and patented a hydrogen sulfide abatement process called AMIS, which is currently the abatement method used in the geothermal power plants of Italy.

The process removes mercury and H₂S from the gases extracted from the condenser by means of an exhauster. The first step is the removal of mercury, where the non-condensable gases are cooled to 70C, suitable for mercury removal by means of specific sorbents, such as sulphurized activated carbon. The next step consists in heating this gas up to around 240C, where a catalytic oxidation of H₂S to SO₂ is carried out. The final step consists in cooling down the non-condensables that exit the oxidation reactor and scrubbing the SO₂ from the gas in a packed column. This process can be achieved without the addition of chemicals, such as sodium hydroxide or ammonia, so long the scrubbing water contains enough ammonia. The clean non-condensable gases are sent to the cooling tower where they are discharged to the atmosphere and the water from the column re-enters the cycle of the geothermal water [49]. The abatement efficiency of the AMIS process is between 75% and 85% for H₂S, with reference to an uncontrolled plant emission. This efficiency takes into

account the fraction of H_2S which is not extracted from the condenser and is dissolved in the liquid stream that leaves the condenser, stream which is not treated by the system [50].

As of December 2012, 26 AMIS plants are in operation, the first of which came online in 2002 and 2003, with 17 more being added between 2005 and 2010. Four additional AMIS plants were built between 2010 and 2012. Six more geothermal plants will be equipped with AMIS treatment plants in the year 2014, which would account for 100% of the total generating plants in the area [51].

2.4.2.8. Non-condensable gas injection systems

In this process, the non-condensable gases are compressed, mixed with the brine and reinjected underground [34].

This same principle is currently used at Hellisheiði geothermal power plant in southwest Iceland. Here, the H_2S is dissolved into water at 90C and pumped down to around 800m where the dissolved gas will mineralize as sulfide metals [5]. This process appears to combine advantages such as low investment, operating and maintenance cost with a high flexibility and no need for wastewater treatment or combustion of exhaust gases as well as no sulfur precipitation or solid disposal. This project is still in a pilot phase. However, it is expected to go on to full production phase in order to meet the new H_2S concentration requirements [5] [34]. Total practical H_2S removal from non-condensable gases is estimated to be about 98% or less [39].

The power plants at the Coso geothermal field in California, operated by California Energy Company, Inc. (CECI) utilized this abatement system for nearly 7 years, but was slowly phased out in favor of other abatement technology in the early to mid 1990's. According to a technical report presented by World Environment Center, [44], the problems encountered during this abatement system's operation included gas breakthrough in BLM field, vapor lock due to insufficient liquid for reinjection and corrosion of the gas lines and well casing. This report concludes that the gas injection method employed in the Coso geothermal power plants was unsuccessful. It is believed that this method will only work effectively for small facilities, for low non-condensable gases concentrations and for lateral injection. In general, it is believed that gas injection is the appropriate abatement method for short-term plant operation. When dealing with long term plant operation, this method can

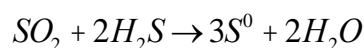
have economic disincentives, particularly with regards to gas leakage in the geothermal field and corrosion problems in pipelines and well casings [44].

In the particular case of the Hellisheiði, the SuFix project is a pilot injection project whose purpose was to investigate the behavior of injecting H₂S as a sequestration procedure. In general, the project aims at assessing the feasibility of H₂S sequestration in basaltic rock by injecting H₂S into the high temperature geothermal reservoir below 800m by dissolving it in hot geothermal water [52]. Predictive simulations were carried out to better understand the performance of this reinjection. The results show that the injected H₂S should be sequestered into pyrrhotite, along with quartz, simple oxides, oxyhydroxides, magnetite, wollastonite and clays. Another study, [22], indicates that the injection of H₂S will increase the reservoir equilibrium concentrations of H₂S, which should result in the mineralization of pyrite and possible other sulfides. Upon mineralization, dilution, heating of the injected water and its mixing with aquifer fluids, it is anticipated that the H₂S reinjected will be sequestered. However, it is important to note that, as [52], “various indications point toward it not being feasible to inject large quantities of CO₂ along with H₂S into deep and hot formations if the objective is to sequester H₂S”. Nonetheless, “the capture and sequestration of CO₂ and H₂S from geothermal power plants is a viable option for reducing their gas emissions, and that basalts may comprise ideal geological CO₂ and H₂S storage formations.” [52]

2.4.2.9. *The Peabody-Xertic Process*

This process, developed by Peabody Process Systems, uses a solution of citric acid to perform an oxidation reaction in liquid phase with solid sulfur as a final product.

The gases extracted from the condenser are separated into two streams, one containing approximately 33% of the total content of H₂S and the other the remaining 66%. The line containing 66% is taken to an agitated reactor where it reacts with a water solution of citric acid and SO₂. The resulting reaction is shown below [53].



Reaction 11: Xertic Process reaction.

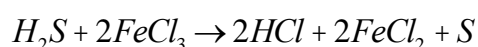
The vent gas from this reactor is sent to an incinerator along with the other stream of off-gases (with 33% content of H₂S) where the H₂S is oxidized to SO₂. From here, the gas is cooled and sent to an absorption tower where a citric acid/sodium citrate solution absorbs the SO₂. The gas remaining from this absorption process is vented to the atmosphere [53].

According to [34] and [53], this method requires high total investment and its operating costs are high. The citric acid solution is also corrosive and therefore there is a need for expensive construction materials.

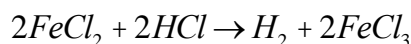
2.4.2.10. The Fe-Cl hybrid method.

This process was first proposed by Japanese scientists in 1991 and [54] has published the results of her lab-scale process.

This method of H₂S abatement utilizes a highly acidic iron solution through which the off-gas from the condenser is bubbled. Solid sulfur precipitates with a nearly 100% turndown of H₂S at solution temperature between 70°C and 75°C. The chemical reactions occurring in this process are shown below in Reaction 12 and Reaction 13 [54].



Reaction 12: Absorption reaction in Fe-Cl hybrid method.



Reaction 13: Electrolysis during Fe-Cl hybrid method.

The separation of elemental sulfur is carried out in a rotary drum vacuum filter. Afterwards, the filtered out solution is taken to an electrolyzer, where the iron solution is regenerated and hydrogen is produced [54].

This method appears to be promising, as [54] points out that this process has the lowest startup costs, fixed capital investment and, of the processes analyzed, is the only one that generates profit. However, it still has only been tested in a laboratory scale and problems may arise with its upscaling. For example, the iron solution is highly acidic, which would require an appropriate material selection, affecting the fixed-capital investment cost greatly. At the same time, the electrolysis cell is not fully developed and the acidic conditions will affect its design. Finally, [54] points out that it is still unknown to what extent the H₂ would be absorbed into the solution. This

will affect the size of the absorption column and solutions, as well as the size of the anode in the electrolysis cell.

2.4.2.11. *Selectox*

A process called Selectox has been used at the Yanaizu-Nishiyama geothermal power station in Japan, which combines the Selectox catalyst with a Claus reaction to produce solid amorphous sulfur [55]. This process consists in three reactors. In the first reactor, the off-gas extracted from the condenser is oxidized using a catalyst based in aluminum oxide and silicon dioxide into SO₂. Then, the SO₂ reacts with H₂S, which has not reacted yet into another oxidation reaction to produce sulfur vapor. The process gas is then condensed and the sulfur vapor produced is removed in a molten state [55].

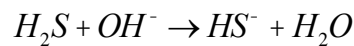
The process gas without the sulfur vapor goes to a second reactor where the H₂S and SO₂ produced in the first reactor oxidize with an aluminum oxide based catalyst to produce more sulfur vapor. This is cooled once again and sulfur is released once more [55].

In the final reactor, the remaining H₂S is oxidized again into SO₂ to prevent the pipelines from clogging. From here on, the process gas is exhausted from the cooling tower [55].

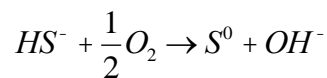
2.4.2.12. *Biological/ THIOPAQ methods*

This process was first developed for removing H₂S from natural gas streams and it involves the use of microorganisms for oxidizing the H₂S to elemental sulfur.

The gas containing H₂S is absorbed in an alkaline solution under pressure in a first absorption step. The dissolved sulfide is oxidized into elemental sulfur in a reactor. The two reactions taking place in this process are shown below [56].



Reaction 14: Absorption reaction in THIOPAQ process



Reaction 15: Oxidation reaction in THIOPAQ method.

The reactor used in this process is patented and varies in design according to the capacity required. Sulfur can be recovered from this process. The elemental sulfur

slurry produced in the reactor can be separated in a centrifuge to various degrees of purity depending on the particular separation configuration [56].

According to [56], this process has minimal chemical consumption and can have a final efficiency of H_2S removal of up to 99.99% with a reactor oxidation to amorphous sulfur between 95% and 98%.

2.4.2.13. Burner-scrubber process

This process consists in incinerating the non-condensable gases from the geothermal fluids. The gases extracted are incinerated and the resulting compounds, mostly SO_2 from the oxidation of H_2S , as well as small amount of CO_2 and water, are scrubbed with water. The sulfur dioxide dissolved in the scrubbing water is returned to the condensate stream. The incinerator can be equipped with a heat recovery system in which water would be converted to steam and then added to the general power plant steam for electricity production [36] [39].

A full-scale prototype of this concept was tested on the Geysers Unit 4 during the late 1970's. Initially, there were problems with the flammability and irregular feed of the gas from the ejectors, but those problems were solved. Much of the H_2S remained in the condensate, rather than being removed with the vent gas to the burner system, so a maximum efficiency of only about 50% was achieved. For this reason, and many other equipment maintenance problems, this system was discontinued [36]. A variation of this process, called the Dow-Spec RT-2, is currently used in some units at The Geysers, as is discussed below.

Strictly speaking, this method is considered to be an “off-gas ejector stream” abatement system, but can be considered a “hybrid” method (Method D, shown below) if the SO_2 scrubbing system is integrated with the cooling tower, whereby both H_2S in the off-gas and the condensate can be removed in the same process. A standalone unit was considered as an abatement method by [39] for the non-condensable gases at Bjarnarflag, Iceland. However, it was concluded that this was not the most economical process for H_2S abatement.

Several studies ([57], [58], [59] and [60]) report that a co-injection of a small amount of SO_2 in the brine is not predicted to cause a rapid and severe brine acidification that would lead to severe corrosion or clogging of the reinjection boreholes. This provides the possibility of the disposal of industrial sulfur-bearing gases in geological formations.

2.4.3. Condensate water (Methods C)

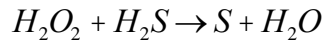
Methods C, also called “secondary abatement”, take place after the condenser and treat the condensed water obtained from this process before the water makes it to the cooling tower. These methods work with both direct contact and surface condensers but the abatement problem is more complicated the case of a contact condenser, as not all the H_2S can be scrubbed in the condensate and so it becomes necessary to treat a stream of condensate as well as the stream of gas collected from the ejector (Methods D, described below).

This section will discuss the following methods:

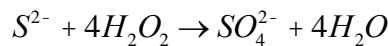
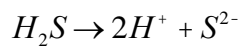
- The H_2O_2 process
- Steam stripping.

2.4.3.1. The H_2O_2 process.

This process consists on extracting the gases from the condenser and scrubbing them in the cooling tower. The water, which now has absorbed a large portion of the non-condensable gases, is treated with hydrogen peroxide to oxidize the H_2S into elemental sulfur (under acidic or neutral solutions) or sulfates (under basic solutions). These reactions, shown below, can occur rapidly in the presence of an iron catalyst [36].



Reaction 16: Acidic environment reaction



Reaction 17: Caustic environment reaction.

This abatement method was used in a demonstration project of an enhanced geothermal system in the Northwest Geysers Geothermal Resource Area [61] to control H_2S emissions during well construction. That process consisted in injecting a stoichiometric amount of aqueous NaOH solution into the pipe used to conduct fluids coming up from the well from the drilling rig (bloeie line) to scrub the H_2S from the steam into a solution as hydrosulfide and sulfide ions. Afterwards, the H_2O_2 would be added to react and oxidize these ions to Na_2SO_4 , which would not revert back to hydrogen sulfide.

2.4.3.2. *Steam Stripping*

This abatement method is analogous to a water scrubbing process, whereby the scrubbing is done by clean steam. Here, the H_2S contained in the condensed water is stripped of H_2S using waste steam from the steam ejectors. Results presented by [62] show that this process is effective under vacuum conditions and at atmospheric pressure, stating that the concentration of H_2S in the treated water was at or below 5ppm under both conditions. The costs of this process should not increase as the concentration of H_2S increases.

2.4.4. Hybrid System (Methods D)

Methods D are hybrid systems, which can perform treatment to both the condensate stream and the gas stream resulting from the condenser stage of the energy production process.

This section discusses:

- Dow-Spec RT-2 process.
- BIOX process.

2.4.4.1. *Dow-Spec RT-2*

This process combines the burner-scrubber process previously described with an iron chelate and is used to treat the off-gas from the ejector and the condensate. As with the burner scrubber process, the H_2S is incinerated to SO_2 , which is scrubbed to form sulfites, which then combines with sulfur from the iron chelate reaction in the circulating water to form soluble thiosulfates. This process is used in Units 5, 6, 7, 8, 11 and 12 at The Geysers, retrofitted to power plants built prior to 1980 [40].

2.4.4.2. *BIOX process*

The BIOX process is another downstream process in which the off-gases are compressed and mixed with the condensate before entering the cooling tower. The oxidizing biocide, in combination with oxygen, converts dissolved H_2S to water-soluble sulfates. This type of oxidation prevents secondary emissions of hydrogen sulfide from the cooling towers [63].

This process was first utilized in 1989 at Unocal's power generating facilities in the Salton Sea geothermal field. Surface condensers coupled to gas ejectors were utilized at that facility at the time and, in 1990, both primary and secondary abatement

were achieved in the plant by compressing off-gas and bubbling it into the circulating water at the bottom of the cooling tower. In 1991 a demonstration testing of this process was successfully conducted at the Bulalo, Philippines geothermal field in a direct contact condenser system using steam gas ejectors and a cross-current flow cooling tower. In this case, like the previous one, both primary and secondary abatement were achieved [63]. According to [64], under optimal operating conditions, “BIOX” agents, such as trichloroisocyanuric acid (TCCA) and bromochlorohydrantoin, are added to circulating water at dosages ranging from 4% to 10% weight of the sulfide present. This can abate H_2S in both surface and direct contact condenser systems.

This process is currently being used in the John L. Featherstone Geothermal Power Plant, also known as the Hudson Ranch I Geothermal Project. The BIOX system removes at least 95% of the H_2S in the non-condensable gases and at least 98% of the H_2S in the condensate used as cooling makeup water. When all of the condensate is used, H_2S emissions from both sources total less than 3.5kg/hr [65]

Similarly, the operation processes detailed in a report issued by the Environmental Management Association, [66], states that this system would be used as the H_2S abatement technique at the Hudson Ranch II geothermal project in California. In this project, it is expected that the BIOX system will remove at least 95% of the H_2S in the non-condensable gases and at least 98% of the H_2S in the portion of condensate used as cooling tower makeup water.

3. Experience at Hellisheiði geothermal plant

The Hellisheiði geothermal power plant is a combined heat and power plant located in southwest Iceland, in a geothermal area known as Hengill. This geothermal area lies in the middle of the western volcanic zone in Iceland, on the plate boundary between North America and the European crustal plates. The rifting of the two plates has opened a North-Northeast system of normal faults and magma intrusions. This rift zone is highly permeable and numerous fumaroles and hot springs emerge at the surface. This is one of the most extensive geothermal areas in the country, with surface measurements, heat distribution and subsurface measurements indicating an area of around 100km² [67].

The purpose of the Hellisheiði power plant is to meet the increasing demand for electricity and hot water for space heating. The power plant was built in modular units, each unit added as the market demand increased. In 2001, the company's board of directors decided to start preparations for building the power plant. The first phase of construction included two high-pressure 45MWe turbines that went online in late 2006 and then one low-pressure 33MWe turbine that went online in 2007. In Fall 2008, two additional 45MWe turbines began operation. The last power expansion went online in 2011 and consisted in two 45MWe turbines [68] [67].

As mentioned before, in response to the public concern as to the unforeseen side effects of H_2S pollution, the Minister of Environment issued Regulation 514/2010, which limits the maximum concentration of H_2S in the atmosphere. In response, Orkuveita Reykjavíkur, the owner of the Hellisheiði power plant, commissioned the construction of a pilot-scale distillation column to explore the possibility of separating the CO_2 and H_2S present in the non-condensable gases as a pre-treatment process of the Carbfix and Sulfix, non-condensable gas reinjection abatement system.

3.1. Conception of the system.

The idea of building a distillation column began before 2008. Feasibility studies were performed on the possibility of abating H_2S by means of conversion to amorphous sulfur (S^0), sulfuric acid, among other possibilities, but there was found to be no market for any of the byproducts produced in these systems. For example, the market value of S^0 was too fluctuating and it was possible for the export costs to be greater than the selling price, making it an economically irrational option. Another possibility looked into was the burial of S^0 , but the its reaction with water, and subsequent formation of sulfuric acid required the combined burial of S^0 with shell sand, which would neutralize the acid formed due to its high calcium content. Once again, this proved to be a rather costly option. In the long run, the distillation method for production of H_2S and CO_2 was viewed as the best option even if it didn't produce any product with immediately tangible market value.

3.2. Operation

The construction of the distillation system began in 2008 and was brought online in Fall 2009. Originally, the system was meant to operate for about 6 months purely as a testing project. As a result, many parts were conceived only as temporary

equipment and therefore the material selected was not meant to handle the corrosive properties of the gas for four or more years, but only for 6 to 12 months. The distillation column itself was built of stainless steel, and so was one of the few equipment designed and built with a longer operating lifespan in mind. However, the welding was not up to standard, so gas started leaking to the heat exchangers and cooling system after a few years of operation, for example.

Another unexpected occurrence was the formation of hydrates in the system. As is explained with more details below, gas hydrates are crystalline water-based solids that resemble ice and occur when water molecules form a cage-like structure around smaller molecules. The main cause of this problem was traced to water accumulation: as water vapor condensed, it accumulated in certain pipes and formed hydrates when in contact with H_2S . This problem could have been avoided if the piping had been designed with certain slope as to drain the water. Since rebuilding the piping was not an option, a dehydration system was installed before the column, which ensured that the gas entering the compressor would be dry, therefore eliminating the possibility of hydrate formation. The solution implemented at Hellisheiði, before the installation of the dehydrator, involved heating the pipeline where the hydrates clogging was believed to be with the purpose of raising the temperature above the critical hydrate formation temperature and melt them. This would be considered a thermal method, as explained further on.

4. Background on the process of Distillation

The previous sections have described various methods for abating H_2S emissions in geothermal power plants. Between them, they provide many geothermal plants, operating in a grand variety of geothermal fields different economically viable and relatively flexible techniques for minimizing gaseous fumes released to the atmosphere. However, none of these seem to be a reasonable alternative for Reykjavík Energy, particularly due to the geographical location of the country. This limits the purchasing of the materials and/or chemicals required for the abatement system, or the possible profit from selling the byproducts of the abatement method.

This is the reason that Reykjavik Energy researched an alternative way for separating the two main component in the NCG stream in the Hengill area: CO_2 and

H₂S. With this process, several alternatives can become available to make the system economically feasible, particularly the stream of purified CO₂.

As has been explored in research papers in different areas [69] [70], there is increasing interest in the possibility of using the purified stream of CO₂ in greenhouses to increase the production of crops grown in Iceland, particularly tomatoes, while reducing the purchasing costs of the CO₂ needed for their growth.

This section discusses some of the technical design criteria to take into account when considering the use of this alternative in H₂S abatement.

4.1. Properties of CO₂ and H₂S

Thermodynamic properties, such as internal energy and enthalpy are necessary for calculating the amount of work or heat required for a particular industrial process. In the case of fluids, these properties can be found using relationships between pressure, volume and temperature. These relationships can provide the foundation for a quantitative and realistic description of the fluid behavior.

4.1.1. PVT behavior of pure substances

A useful way of depicting the phases that can occur at equilibrium in a pure substance is with the use of a phase diagram. A phase diagram consists of lines of equilibrium, or phase boundaries, which mark the conditions under which multiple phases coexist in equilibrium. This is where phase transitions can occur given a change of temperature, pressure or both. The point where the lines of equilibrium intersect is known as triple point. This point marks the conditions at which the substance's solid, liquid and gaseous state can coexist in equilibrium.

4.1.2. Carbon dioxide phase diagram

Figure 2 below shows the phase diagram for pure carbon dioxide. As explained before, these lines of equilibrium mark the conditions under which multiple phases can coexist in equilibrium. Line A is the sublimation curve and it separates the solid and gas regions. Line B is the fusion curve and separates the solid and liquid regions. Line C is the vaporization curve and separates the liquid and gas regions. The critical point, with coordinates (P_c , T_c), is the point with the highest pressure and highest temperature at which the CO₂ is observed to be in gas/liquid equilibrium. The triple point is the point in which the three phases coexist in equilibrium. The triple point is

invariant for any given pure substance, meaning it will only occur at the given pressure and temperature [71].

For carbon dioxide, the critical point is 31°C. Above this temperature, the gas cannot be liquefied regardless of the pressure applied. Liquid carbon dioxide can only exist between the triple point temperature and the critical point temperature (21.05°C and 31°C) and pressures between 517.8 kPa and 7349.7 kPa., its triple point and critical pressure.

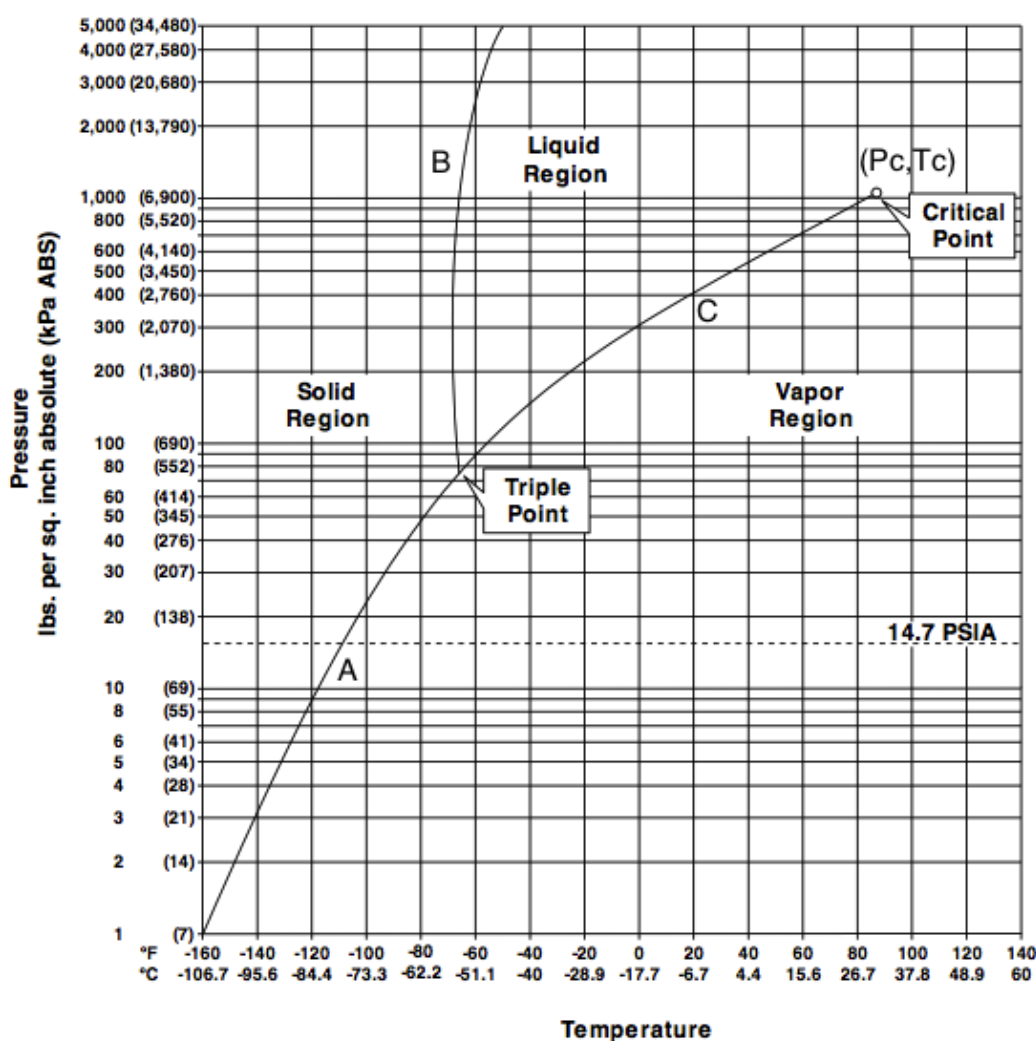


Figure 2: Carbon dioxide phase diagram

4.1.3. Hydrogen sulfide phase diagram

A complete phase diagram for hydrogen sulfide was not found in the literature. Figure 3 was plotted using data from [72] and it presents the vaporization curve, which separates the liquid and gas regions of the hydrogen sulfide. The critical point, labeled as A, is the last point shown in that figure. For pure hydrogen sulfide, this

point occurs at 99.95°C and 88.82atm, or 8.99MPa. The triple point of the gas, not shown in the Figure due to its scale, is located at 0.02MPa and -85.45°C.

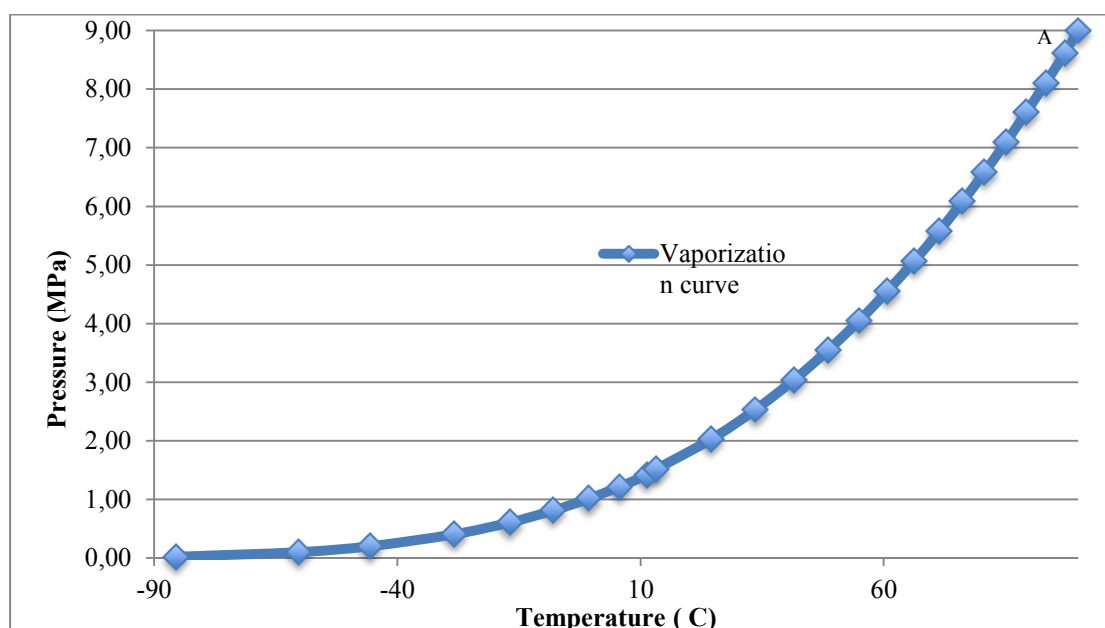


Figure 3: Vaporization curve of pure H₂S phase diagram.

4.1.4. Binary Vapor-Liquid-Equilibrium

Equilibrium is a static conditions in which no changes occur in the macroscopic properties of a system. In practical terms, the assumption of equilibrium is justified when the analysis of the system leads to results of satisfactory accuracy. An isolated system consisting of liquid and vapor phases eventually reaches a final state where there is no tendency for change to occur.

Vapor liquid equilibrium (VLE) is a state where liquid and vapor phases coexist in a way where the rate of evaporation equals the rate of condensation such that there is no overall vapor-liquid interconversion. A mixture at VLE is referred to as a saturated fluid. The concept of “saturated fluid” includes saturated liquid (about to vaporize) and saturated vapor (about to condense). Such VLE information is useful in designing distillation columns [71].

Table 4, shown below, provides the VLE data for a system composed of CO₂ and H₂S at 40bar. Using this information, it is possible to plot the VLE curve for this system, shown in Figure 4 below. Table 5 shows the VLE data for the same system at 20bar, while Figure 5 shows the plot of the VLE curve for the system.

Table 4: Binary Vapor-Liquid Equilibrium Data for CO₂-H₂S System at 40bar [73]

Temp. (°C)	X (%mol)	Y (%mol)
54.99	0.000	0.000
50	0.035	0.124
45	0.074	0.216
40	0.117	0.300
35	0.168	0.382
30	0.232	0.467
25	0.313	0.546
20	0.420	0.630
15	0.563	0.720
10	0.756	0.835
9	0.797	0.862
8	0.852	0.899
7	0.916	0.942
5.80	1.000	1.000

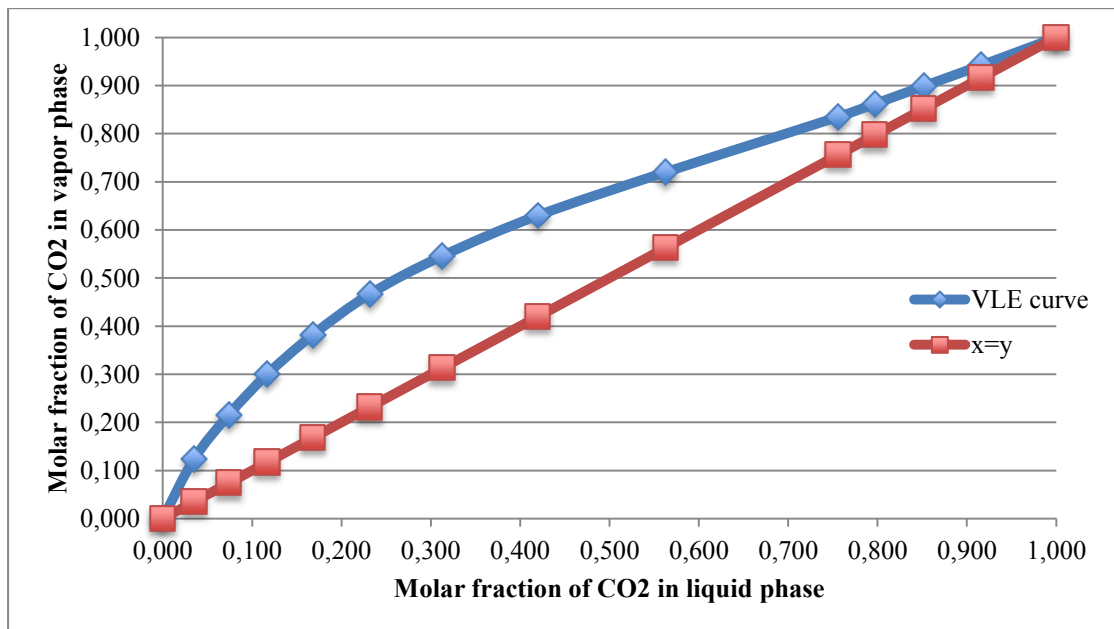


Figure 4: VLE curve for CO₂-H₂S System at 40bar

Table 5: Binary Vapor-Liquid Equilibrium Data for CO₂-H₂S System at 20bar

Temp. (°C)	X (%mol)	Y (%mol)
24.5	0.000	0.000
20	0.020	0.131
15	0.052	0.240
13	0.092	0.341
5	0.142	0.441
0	0.211	0.531
-19.08	1.000	1.000

4.2. Distillation

Distillation is a method for separating mixtures based on differences in the volatility of the components in the mixture. When a liquid mixture is heated, the vapor that comes off will have a higher concentration of the more volatile material. This difference in concentration results in a separation between the components. Conversely, if a vapor is cooled, the less volatile material will have a tendency to condense in a greater proportion than the more volatile material [74] [75].

4.2.1. General principles of distillation

The distillation process uses a cylindrical shell that holds inside random or structured packings and plates that are used to contact together the liquid and gas phases of the mixture. The material is fed at one point along the column, sometimes more. The liquid will run down the column while the vapor flows upward. The liquid that reaches the bottom of the column is partially vaporized in a heated reboiler to provide what is known as a boil-up. As the boil-up makes its way up the distillation column,

the lighter elements in the mixture will tend to concentrate in the vapor phase, while the heavier ones will concentrate in the liquid phase. Once the vapor phase reaches the top of the tower, it is cooled and condensed in the overhead condenser. Part of this liquid can be returned to the column to provide liquid overflow [74] [76].

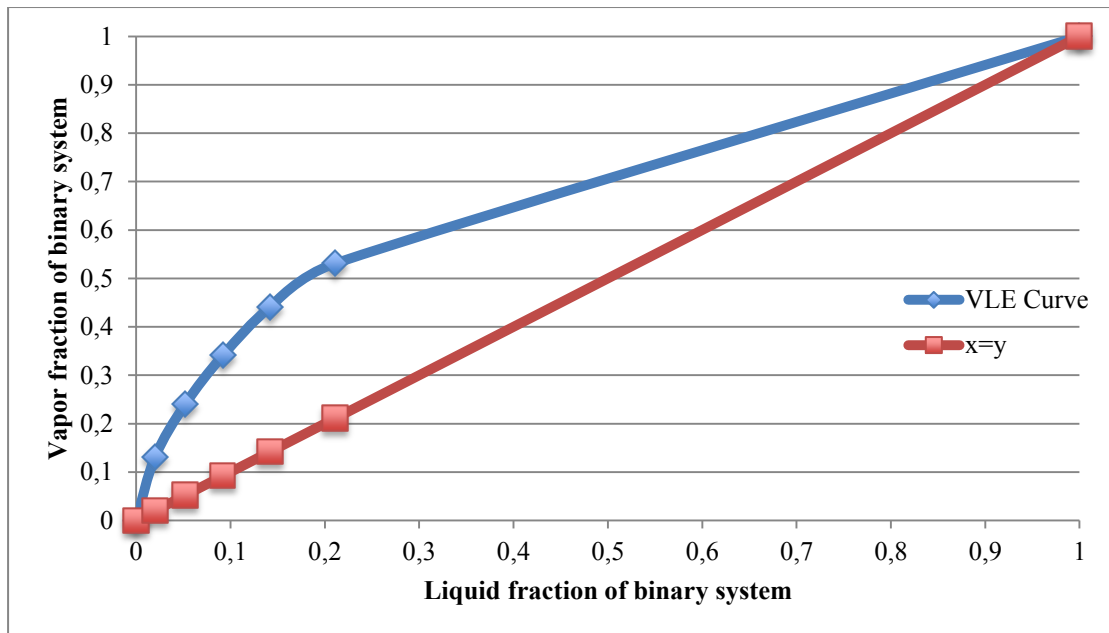


Figure 5: VLE curve for CO₂-H₂S system at 20bar

All distillation operations require energy to separate the species. In the most conventional distillation operation, this energy is provided in the form of heat to the reboiler, at the bottom of the distillation column. Heat must also be removed at the top of the equipment (the condenser) [74].

4.2.2. Cryogenic distillation of gases.

Cryogenic distillation is similar in principle to ordinary distillation. However, this process takes place at extremely low temperatures. For example, the process for separating air into its basic components (oxygen and nitrogen, mainly), the process needs to be carried out at around 100 K. In these cases, nitrogen is the most volatile component and will be the one present in highest concentration in the top of the column. For the condensation portion of the distillation column, it would become necessary to use a cooling medium with a lower boiling point than nitrogen, which would pose a problem since a very costly installation would be required to achieve these low temperatures [77]

4.2.3. Liquefaction

Any liquefaction process will require the gas to be refrigerated at some temperature below its boiling point and below its critical temperature so that the liquid can condense at a pressure below the critical pressure. Gas liquefaction is a special case of gas refrigeration and thus shares the basic principles of refrigeration,

which are as follows. The first step is to compress a gas while it is thermally connected to a heat sink so that any excess in temperature can be dumped into it. After moving the gas to a different location, it is expanded while it is thermally isolated, causing it to cool. This gas can then be moved to a different location and be thermally connected to the object to be refrigerated. After absorbing the heat from this object, it is removed from it and sent to a different location where it is returned to its original temperature [78].

There exist a large number of refrigeration cycles that use different combinations of heat rejection, absorption and gas expansion and compression, like Joule-Thomson, Stirling, Brayton, Claude, Linde, Hampson, Postle, Ericsson, Gifford-McMahon and Vuilleumier. The so-called “regenerative cycles” (Solvay, Postle, Gifford-McMahon, Ericsson, Stirling and Vuilleumier) do not depend significantly on the operating fluid, provide cyclic operation (fluctuating cold temperatures), have moving parts at low temperatures and tend to be smaller and lighter than “recuperative cycles”. These “recuperative cycles” include Joule-Thomson, Claude and Brayton cycles. These are characterized because they depend heavily on the operating fluid, produce even (not cyclic) cooling and will be bigger and heavier than their regenerative counterparts because they operate at higher pressures. These cycles tend to be used for larger scale operation while the regenerative cycles are used for smaller applications [78]

4.2.4. Liquefaction methods.

This section presents the general operating principles of the most useful liquefaction methods.

4.2.4.1. Vapor compression.

The vapor compression process uses a circulating liquid refrigerant as the medium that absorbs heat from the surroundings and eventually rejects it to a heat sink. The refrigerant enters the compressor as a saturated vapor, is compressed to a higher pressure where it raises its temperature. It then flows through a heat exchanger, where it rejects heat from the system. The condensed, saturated liquid that results goes through an expansion valve where it reduces its pressure. This sudden reduction in temperatures leads to an adiabatic flash evaporation of part of the refrigerant. This

lowers the temperature of the liquid to where it is colder than the temperature of the space to be refrigerated. The mixture is then sent to an evaporator, where it returns to its original state as saturated vapor and routed back to the compressor [78].

4.2.4.2. Cascade vapor compression

A cascade vapor compression system consists in a series of compressors, evaporators and condenser, each containing different refrigerants. Each system is connected to the next one by a heat exchanger, which acts like an evaporator for one cycle and as a condenser for the other cycle. Through this mechanism, the heat released by the second refrigerant as it condenses is absorbed by the refrigerant in the first cycle, causing it to evaporate [78]

4.2.4.3. Mixed refrigerant cascade method.

A variation of the cycle described above involves the circulation of a single refrigerant prepared from a mixture of refrigerants. Under certain circumstances, this variation may provide a reduction in capital expenditure over a conventional cascade cycle. A variation of this method used in very large natural gas liquefaction plants involve a multicomponent mix that is repeatedly partially condensed, separated, cooled, expanded and warmed again as the refrigerant makes its way through the natural gas liquefaction process [78].

4.2.4.4. Linde refrigerator

A simple Linde cycle starts with the gas compressed at ambient temperature, rejecting heat to a coolant so the process stays approximately isothermal. The compressed gas is then cooled in a heat exchanger until it reaches a throttling valve. Upon expansion, the gas is cooled until a portion of the gas liquefies. Liquid nitrogen is normally used as the refrigerant for hydrogen and neon liquefaction systems, whereas liquid hydrogen is the normal refrigerant for helium liquefaction systems [78]

4.2.4.5. Stirling

As with most other heat cycles, this one comprises of four main processes: compression, heat addition, expansion and heat removal. The idealized Stirling cycle consists on an isothermal expansion of the gas, which undergoes a near-isothermal expansion. Next, at constant volume, the gas is cooled and the heat extracted is used

for the next cycle. The next stage is an isothermal compression. Finally, the compressed air flows back through a regenerator picking up the heat removed in the second stage and the whole cycle begins once again [78].

4.3. The McCabe-Thiele design method.

In practice, distillation can be carried out with two main methods: flash distillation and continuous distillation. Flash distillation consists in vaporizing the liquid mixture thorough boiling and condensing the vapors without allowing the condensed liquid to return to the distillation equipment. The second method, continuous distillation, is based on the return of part of the condensate into the distillation column. Flash distillation is not efficient in the separation of components with comparable volatility, which require continuous reflux from the distillation tower. The McCabe-Thiele method is a graphical method used to calculate the number of ideal plates required for a given mixture to reach desired end-product concentration [71]. The following sections provide a simplified description of this method.

4.3.1. Mass Balance

Figure 6 is a mass balance diagram of a typical continuous distillation column. The column is fed F mol/h of mixture with concentration x_F and distills D mol/h of product with concentration x_D and B mol/h of bottom product with concentration x_B . Two material balance equations can be written:

Equation 1: Total mass balance

$$F = D + B$$

Equation 2: Component A balance

$$Fx_f = Dx_D + Bx_B$$

From these equations, the following equations can be derived:

Equation 3: Mass balance independent of B

$$\frac{D}{F} = \frac{x_F - x_B}{x_D - x_B}$$

Equation 4: Mass balance independent of D

$$\frac{B}{F} = \frac{x_D - x_f}{x_D - x_B}$$

4.3.2. Feed and Operation and lines.

For the Feed line, it's necessary to define a factor q as the moles of liquid that flow in the stripping section that result from the introduction of 1 mole of feed. The value of q for a cold-liquid feed is found from Equation 5, shown below, where C_{pL} is the specific heat of the liquid, T_F is the feed temperature, T_B is the bubble point of the feed and λ is the enthalpy of vaporization of the mixture [71].

Equation 5: Equation for q

$$q = 1 + \frac{C_{p,L}(T_b - T_F)}{\lambda}$$

The Feed line can then be represented as a straight line, with the following equation [71]:

Equation 6: Feed Line equation

$$y = -\frac{q}{1-q}x + \frac{x_F}{1-q}$$

The Rectifying line is drawn as the line that intercepts the y -axis at the point $x_D/(R_D+1)$, where R_D is the reflux ratio, and the point x_D, x_D . On the other hand, the Stripping line is the line that passes through the point (x_B, x_B) and the intersection of the Rectifying line with the Feed line.

Regarding the heating and cooling requirements of the system, if steam is used as a way of providing heat, then Equation 7 can be used to quantify the steam consumption required for the process and Equation 8 can be used as the cooling water requirement in the condenser [71].

Equation 7: Vapor requirement

$$\dot{m}_s = \frac{\bar{V}I}{I_s}$$

Equation 8: Cooling water requirement

$$\dot{m}_w = \frac{VI}{T_2 - T_1}$$

, where \dot{m}_s and \dot{m}_w are the mass flow rates of steam and water, respectively, \bar{V} is the production rate of steam in the reboiler, I and I_s are the vaporization enthalpy of the mixture and steam, respectively and $T_2 - T_1$ is the temperature difference in the cooling water.

The graphical process continues as follows. On the VLE diagram, a diagonal line is drawn from the origin of the xy -axis to the point (1,1). As stated before, the Rectifying line is drawn from the point (x_D, x_D) to the point $(0, x_D/(R_D+1))$. The Feed line is drawn from the point (x_F, x_F) upward with a slope of $(-q/I-q)$ and the Stripping line is drawn from (x_B, x_B) to the intersection of the Rectifying line and Feed line. After all these lines have been plotted, the number of ideal plates is found by a step-by-step construction, which can either start at the bottom of the Stripping line, or at the top of the Rectifying line. If the construction begins at the top, then the first stage is a “step” starting at the point x_D , horizontally straight until it hits the VLE line, then vertically down until it hits the Rectifying line.

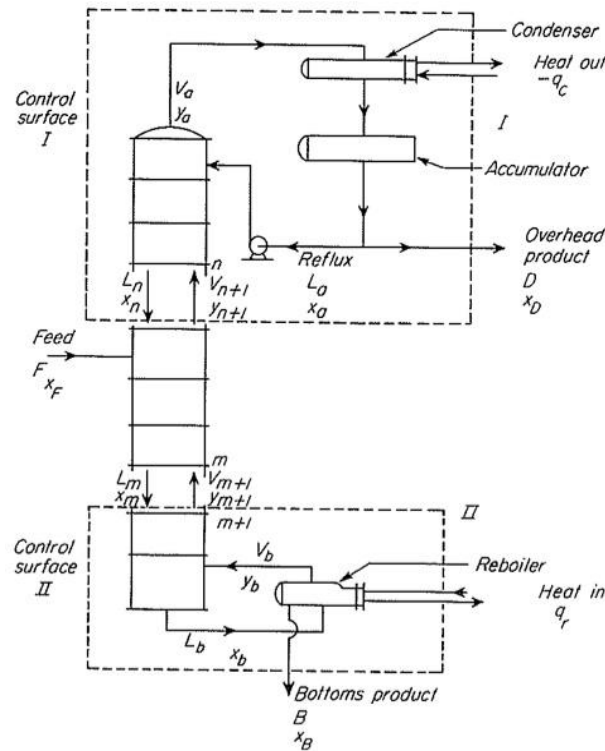


Figure 6: Mass balance for distillation column

This step is repeated until the intersection of the operating lines is approached. At this point, after the “step” crosses the intersection of the Rectifying and Stripping lines, a change should be made such that the “step” reaches the Stripping line in a manner that the maximum enrichment per plate is obtained. Figure 7 gives an

illustration of the step-by-step procedure described here. That same figure shows that maximum enrichment per plate is reached if the “step” changes from the Rectifying line to the Stripping line. The feed plate of the tower is represented by the triangle that has one corner on the Rectifying line and one on the Stripping line.

5. Clogging risks associated with gas hydrates

One of the challenges facing processes that involve water and small, non-polar molecules is the formation of gas hydrates, as explained by the experience at the Hellisheiði power plant. The avoidance of this problem is key in assuring the correct flow throughout the equipment enabling the design of an optimum production system. Prevention of gas hydrates plugs is often the key strategy in assuring normal flow conditions and often the most expensive to implement [79].

5.1. Gas hydrates

Gas hydrates are crystalline water-based solids that resemble ice and occur when water molecules form a cage-like structure around smaller, usually non-polar, molecules. In these cases, the water is said to be the host molecule while the guest molecule is typically a gas. The most common guest molecules are methane, ethane, propane, isobutene, n-butane, nitrogen, carbon dioxide and hydrogen sulfide, although other low-molecular weight gases such as oxygen and hydrogen can form hydrates under suitable temperatures and pressures.

The two major conditions that promote hydrate formations are the gas being at the appropriate temperature and pressure and the gas being at or below its water dew point. Other factors that can facilitate hydrate formation include mixing, kinetics, surface for crystal formation and salinity. These hydrates are not chemical compounds, as the sequestered molecules are never bonded to the water molecules, nor the process of formation is a chemical reaction, but rather a first order phase transition [79] [80] [81]

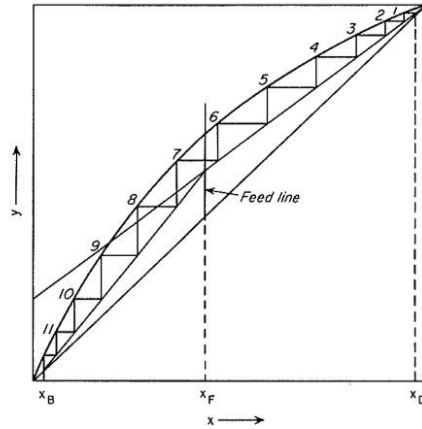


Figure 7: Drawing of number of ideal steps with McCabe-Thiele method.

5.2. Clogging prevention techniques.

Since gas hydrates are water-based solids, a permanent solution would be to remove water for any type of process that could potentially produce hydrates. Another technique would be to avoid the regions of temperature and pressure where hydrates can form. These options would depend on each specific process, as there may be some constraints regarding these operating parameters. In general terms, there are two types of methods applicable for preventing formation of hydrates [79].

5.2.1. Thermal methods.

Thermal methods consist simply in the conservation or addition of heat in order to maintain the mixture outside of the hydrate formation range. Again, this will depend extremely on each particular process, as the process itself may have specific temperatures. If this is not a limitation, heat conservation can be a useful technique involving simple insulation. As with any design project, such insulation system will seek to balance cost and risk. Another simple solution might be the installation of a hot water jacket surrounding the process equipment [79].

Urdahl, et al., [82] present their operational experience of applying direct electrical heating for hydrate prevention in multiphase pipelines on the Norwegian Continental Shelf. That paper explains how the Huldra-Veslefrikk pipeline was the first pipeline to be put in operation with a direct electrical heating as the primary hydrate prevention method. Direct electrical heating heats the pipeline by forcing a large electric current to flow through the pipeline steel. The system is used primarily for hydrate prevention rather than hydrate plug removal. Although this procedure is theoretically possible, the operability window is extremely restricted due to the risk of

pipeline rupture caused by varying melting rates along the pipeline, which increases the risk for critical pressure build-up.

5.2.2. Chemical methods.

Chemical methods consist in using chemical inhibitors, which are injected in the equipment and prevent hydrate formation by depressing the hydrate temperature below that of the equipment's operating temperature. However costly this method can be, it can still be more economical than some thermal strategy and it is still the most widely used method in the oil and gas production industry, where the formation of natural gas hydrates is a serious problem [79]

5.2.2.1. Thermodynamic inhibitors

The most common chemical additives used have been methanol, ethylene glycol or triethylene glycol. When added, these chemicals have the effect of displacing the hydrate formation area to a point of lower temperature and/or higher pressure. A primary factor in the selection process is whether or not the chemical can or will be recovered, regenerated and re-injected. For example, methanol is considered a non-regenerable chemical and is usually preferred because of its low viscosity and surface tension. Glycols are considered to be a costly chemical inhibitor since they sometimes need to be added in approximately the same amount of the weight of water. This means that any chemical inhibition strategy involving glycols would need the construction of a regeneration facility [79]. In general terms, the effectiveness of these inhibitors is well known, but large concentration are needed, which can impact project economic studies [83].

5.2.2.2. Kinetic inhibitors.

The kinetic inhibitors are high molecular weight polymers, which prevent crystal nucleation or growth inside equipment. These inhibitors should be considered for short residence times, in the order of a few minutes [79].

A study presented in 1995 [84] showed a second generation of kinetic inhibitors of the family of lactam-ring polymers. These inhibitors are PVCAP (poly(N-vinylcaprolactam)), VC-713 (N-vinylpyrrolidone/N-vinylcaprolactam/N,N-dimethylaminoethylmethacrylate) and VP/VC (N-vinylpyrrolidone-co-N-vinylcaprolactam).

A first-generation inhibitor called PVP (polyvinylpyrrolidone) was proven to be effective but at temperatures around 285K. When the temperature decreased to 277K, PVP enabled hydrates to form more plentifully. Studies performed on the second-generation kinetic inhibitors presented above have shown they are superior to PVP at 6.7 MPa. Lederhos, *et al.* [84] shows that at high pressures (10.3MPa), VC-713 fails to inhibit massive amounts of hydrates. However, at moderate pressures, VC-713 was shown to delay large amounts of hydrate formation for at least 20 hours. The results in the experiments also showed that the amount of this inhibitor was an important factor in preventing or delaying the formation of hydrates.

On the other hand, PVCAP allowed small formation of hydrates at less than 6.9 MPa but was ineffective at 10.3 MPa. For this particular inhibitor, it was shown that the presence of salt water had an optimal inhibition performance at 6.9 MPa. As with VC-713, PVCAP was also tested at different concentrations [84].

The commercially available VP/VC inhibitor was studied with different ratios of vinylpyrrolidone and vinylcaprolactam. It was shown that when the ratios of VP/VC were equal or less than 25/75, the inhibitor was as effective as either PVCAP alone or VC-713 [84]

Koh, *et al.*, [85] also presents experimental results comparing PVP and VC-713 in tetrahydrofuran (THF) hydrates. For a mixture containing a mole ratio of THF/water of 17:1 and 27:1, VC-713 appears to have more inhibition power. VC-713 is effective at controlling the onset of hydrate formation in both mixtures, whereas PVP is only effective at induction control in dilute solutions.

5.2.2.3. *Anti-agglomerant inhibitors.*

Anti-agglomerators, on the other hand don't inhibit hydrate formation, only hydrate plugging. They allow hydrates to form but keep the particles small and the viscosity low enough so that the hydrates flow dispersed [79].

Koh *et al.*, [85] studied the inhibition capacity of a commercially available quaternary ammonium bromide (QAB). As mentioned before, the study involves the use of a THF hydrate with mole ratios of 17:1 and 27:1. In their results, QAB shows better control of the rate of hydrate formation after nucleation. For the samples of mole ratio of 17:1, QAB performed in between PVP and VC-713, but its inhibition power increased for the 27:1 samples, outperforming both PVP and VC-713. This

quaternary ammonium bromide anti-agglomerant inhibitor is ineffective at hydrate nucleation control. However, it exhibits excellent hydrate growth control in 27:1.

Huo, *et al.*, [83], worked with commercially available surfactants and synthesized anti-agglomerants and found that some of the surfactants (Span 20, Span 40, Span 60, Span 80) could keep hydrate particles suspended at 8.27 MPa. With regards to synthesis anti-agglomerants, many lactam-ring-based chemicals and some chemicals with other functional groups were also efficient in preventing hydrate plugging. The most efficient one used, (dodecyl-2-(2-caprolactamyl)ethanamide) was the more efficient dispersant at 0.75 wt% of the water mass.

Kelland, Svartas and Andersen [86] discusses new types of anti-agglomerants, which are based on surfactants with a high degree of propoxylation. Their experiments show that polyamine polypropoxylates and other branched polypropoxylates are able to disperse gas hydrates in a synthetic natural gas fluid as long as there is good agitation. However, linear, unbranched or low molecular weight polypropoxylates did not perform well, as well as other classes of surfactants, such as anionic and various polyethoxylated surfactants. They also found that the addition of kinetic hydrate inhibitors such as PVCAP reduces the performance of polyamine polypropoxylates as anti-agglomerants.

6. Results and discussion

6.1. Section with results regarding abatement methods.

One of the purposes of this thesis work was to explore some of the most widely used H₂S abatement methods in the industry in an attempt to bring together the experience accumulated over the years. Alongside this, it also attempts to serve as a decision tool for choosing appropriate abatement methods for different geothermal plant and geothermal field conditions.

A literature research was performed in order to review the most common abatement methods, their characteristics, advantages and limitations. A preliminary evaluation of the initially selected methods was carried out. Table 6 presents the data in a condensed form with their criteria employed for their evaluation.

Regarding the Copper Sulfate process, it was found that, despite being able to use both type of condensers and with a high H₂S removal efficiency, its high capital and operating costs make it an undesirable choice for H₂S abatement purposes. On the other hand, the Scrubbing with alkali process can also be installed with both type of condensers and it is not influenced by the geothermal steam composition. Its low capital and relatively high operating costs make it suitable for small power plants, with small operating lifespan.

The liquid redox methods can only use surface condensers but have very high removal efficiency of the H₂S entering the stream. The concentration of ammonia in the geothermal steam must be low (NH₃-to-H₂S ratio below 1) because a high concentration of this compound promotes dissolution of hydrogen sulfide in the water phase. Given the complexity of the majority of the processes in this category, a high capital expense is required, but they usually have a very low operating cost. For this reason, these processes are best suited for large units, with an extended operating period. On the other hand, the AMIS process operates well with a direct contact condenser and low ammonia content in the geothermal steam. It is currently used in small plants, but the process has been tailored for the particular composition of the Italian geothermal steam. The non-condensable gas injection system can use only surface condenser and has a large H₂S removal efficiency. The relative simplicity of the process gives it low capital and operating costs, which makes it a candidate for application in both large and small geothermal plants. The Peabody-Xertic process

can only use surface condensers and is subject to the geothermal steam having low concentration of ammonia. The high capital and operation costs of this system eliminate the possibility of its viability in small power plants, therefore it is only recommended for large projects, with extended operating periods. Another off-gas ejector steam method is the Fe-Cl hybrid system, which appears to be quite promising, as it has low capital and operating costs. However, the process is still in laboratory scale experimentation and it is unknown how the system will behave in commercial applications. The Selectox process uses direct contact condensers and works with low ammonia content in the steam. It is recommended for use in relatively large units as its complexity requires high capital costs, but offers low operating costs. The THIOPAQ method was found to be only used in the gas industry and still in need to be researched and adapted to geothermal power plant conditions. Finally, the burner-scrubber process was found to be able to operate with both types of condensers, although direct contact was preferred. Its operation is strongly dependent on the composition of the geothermal steam, specially regarding the concentration of ammonia. If the geothermal steam has low NH_3 concentration, then the process is characterized by having high capital costs but low operating costs, making it more suitable for large plants. However, if the NH_3 content is high, the process has low capital costs but high operating costs, making more suitable for small geothermal units. As mentioned in [36], this process relies on the non-condensable gas composition, particularly the concentration of flammable gases, such as H_2S and H_2 . An irregular flow of combustible gases from the ejectors can lead to marginal flammability and an intermittent operation of the burner. If these problems require the additional input of fuel to burn the gas, the economic conditions of this abatement system may become unfavorable for this to be an abatement option.

Regarding the condensate water methods, the H_2O_2 process can operate well with both type of condenser but it requires a high concentration of ammonia, as this favors the dissolution of H_2S in the aqueous phase. It has low capital costs but high operating costs, mainly due to the amount of chemicals used in the process, so it is best suited for small units or certain short-term operations, such as during well construction. The other condensate method, Steam stripping, can also be installed with both types of condensers and is effective with low ammonia concentration. Its high capital and low operating costs make it ideal for use in large power plants.

The Dow-spec RT-2 process was found to be currently used in plants with direct contact condensers and low-to-medium NH_3 concentration. Operational costs were found to be similar to systems best suited for large plants [40]. For this reason, it's reasonable to expect this process to be best suited for large plants. Finally, the BIOX process can be used in power plants installed with both types of condenser and is unaffected by the concentration of NH_3 in the steam. The process does not require high capital and operating expenses, making it proper for installation in both large and small power plants.

As can be seen from this brief analysis, each abatement process has its own characteristics and advantages and disadvantages, making the problem of selecting one somewhat complicated. By excluding the processes presented in Table 6 that presented the most negative characteristics in regards to the condenser design required, the type of geothermal steam or whether they were favorable economically or not, the recommended methods were narrowed down to eight. The results are summarized in Table 7. Methods C (abatement from the condensate water), also called "secondary abatement" were used as complimentary processes of those processes that are viable but have a rather low overall efficiency, like the liquid redox and NCG injection methods, which depend on selectivity of H_2S to stay in the gaseous phase, rather than dissolving in the condensate water.

As can be seen in Table 6, the Scrubbing with alkali and BIOX processes appear to be the most flexible because both types of condenser in a geothermal plant can be used and the geothermal steam does not influence them. This is particularly beneficial as a change in the geothermal steam composition can be expected throughout the operational lifespan of a geothermal power plant.

Both the NCG injection and BIOX processes share the fact that they are the only ones with low expected capital and operation costs. This makes them suitable for treatment of H_2S emissions in both large and small power plants, but the BIOX process performs better with regards to the condenser design and ammonia content criteria.

On the other hand, the liquid redox, selectox and steam stripping methods have a complex process, which causes them to have high capital costs, making them more suitable for large units. However, the steam stripping method appears to have a

comparatively low H₂S removal efficiency, limiting its usefulness to being used only in combination with other abatement systems.

The Scrubbing with alkali and the H₂O₂ processes have in common the fact that they are simpler than the two processes previously mentioned and so don't have a high initial investment cost. However, they do present higher operating costs, which limit them to smaller power plant application. However, like the steam stripping process, the H₂O₂ process has a lower H₂S abatement efficiency, limit further its use as only appropriate in combination with other abatement processes.

The off-gas ejector system processes selected (Stretford, Unisulf and LO-CAT), alongside the NCG injection and Selectox are strongly dependent on the concentration of ammonia in the geothermal steam. Therefore, adoption of these systems requires taking into account not only the use of surface condenser in the geothermal plant, but the geothermal system. As has been mentioned before, the fact that they are strongly dependent on this composition is a rather large setback, as it is well known that this composition can vary along the lifetime of the geothermal plant.

Finally, it is the BIOX process that seems to provide the most benefits and fewer disadvantages of the systems analyzed. However, it must be stated that these processes must be subjected to a more rigorous and detailed technical and economical analysis.

Figure 8, shown below, attempts to serve as a decision tool for choosing appropriate abatement methods for different geothermal plant and geothermal steam compositions. It is a basic outline designed to provide a quick, graphical summary of the methods selected from the total number of presented in the literature review.

Table 6: Criteria used for preliminary selection of H₂S abatement processes.

Process	Condenser Design	NH ₃ /H ₂ S ratio	Economics	Best suitable for	Comments
Copper sulfate	DCC and SC	High	High cap. & op. costs		Not recommended
Scrubbing with alkali	DCC and SC	Both	Low cap & relatively high op. Costs	Small plants	
Liquid redox methods.	SC	Low	High capital costs	Large plants	
AMIS	DCC	Low		Currently applied in small plants in Italy	Process more or less tailored for Italian field characteristics
NCG injection	SC	Low	Low capital operational costs.	Small and large plants	
Peabody-Xertic	SC	Low	High cap. And high op. Costs	Large units	
Fe-Cl hybrid					Still a lab. Scale process
Selectox	DCC	Low	High cap. Cost and low op. Costs	Medium to large plants	Used in 65MW plant in Japan
Biological/THIO PAQ					Needs to be adapted from gas industry
Burner-scrubber	SC and DCC	Both high and low	High NH ₃ content: High cap. And low op. Costs Low NH ₃ content: Low cap. And high op. Costs	Low NH ₃ : Large units High NH ₃ : Small units	DCC preferred.
H ₂ O ₂ process	SC and DCC	High	Low cap. Costs and high op. Costs	Small units	Recommended only as secondary abatement.
Steam stripping	SC and DCC	Low	High cap. Costs and low op. Costs	Large units	
Dow-Spec RT-2	DCC	Low to med	High capital costs.	Large units	
BIOX	SC and DCC	Both	Low cap and op costs	Small and large	

DCC: Direct Contact Condenser

SC: Surface Condenser

Table 7: Summary of recommended H₂S abatement methods

Method	Comments
Scrubbing with alkali	Recommended for small units
Liquid Redox methods	Specifically the following: Stretford, Unisulf, LO-CAT II. Has limitation regarding the condenser design but can be used in combination with H ₂ O ₂ process or steam stripping
NCG injection	As with the liquid redox methods, has limitation regarding the condenser design but can be used in combination with H ₂ O ₂ process or steam stripping.
Selectox	Has limitation in the required condenser design.
Dow-Spec RT-2	Has limitation in the required condenser design.
BIOX	Combines flexibility in condenser, ammonia content and expenses.

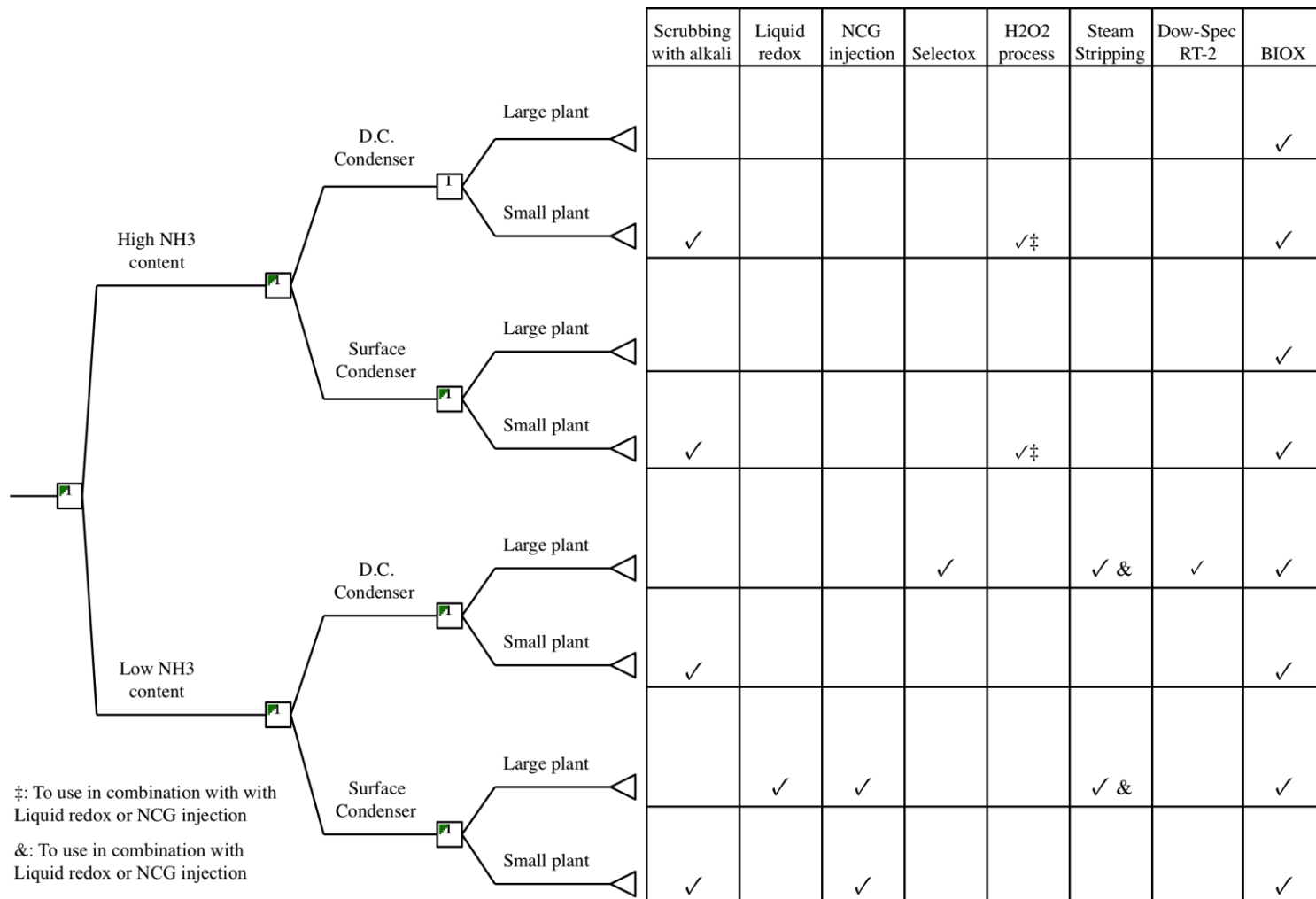


Figure 8: Proposed H2S abatement system selection decision tool

6.2. Section with results regarding distillation

One of the purposes of this thesis work was to explore one subset of the many H₂S abatement process, namely, the distillation of both CO₂ and H₂S and at the same time, provide the design of a small scale distillation system, with modular-form design, with the intent of providing a framework for implementing a large scale pilot operation of this abatement method.

The designing process requires the selection of a design basis around which to design the process and the equipment. Table 8 shows the criteria used for this particular process. These conditions were selected on the basis of the actual conditions under which the distillation tower at Hellisheiðarvirkjun operated.

Table 8: Design basis for distillation process.

Condition	Basis
Pressure	4MPa/2MPa
Temperature	-20C
Flow	20kg/h
Concentration of CO ₂ in feed	0.7876 % w/w
Concentration of CO ₂ in distillate.	0.97 % w/w
Reflux ratio	3.5

The method chosen for determining the number of ideal plates was the McCabe-Thiele graphical method. As shown in a previous section, this process requires a mass balance performed with regards to the overall flow in the column as well as a balance regarding component A, which in this case is CO₂. For a hypothetical flow of 20kg/h of gas mixture feed and a CO₂ concentration in the distillate of 97% w/w, Table 9 shows that the flow of distillate is expected to be approximately 0.369 kmol/h while approximately 0.113 kmol/h will flow in the bottoms section. In these streams, the CO₂ concentration of the gases emitted to the atmosphere is expected to be 0.962%mol and 0.023%mol in the stream at the bottom of the distillation tower.

Table 9: Simplified mass balance for distillation process.

Location	Flow (kmol/h)	%mol CO ₂
F	0.483	0.742
D	0.369	0.962
B	0.113	0.023

As discussed in section 4.3.2, the McCabe-Thiele method requires the drawing of Feed and Operational lines. The appropriate drawing of these lines require calculating certain thermophysical properties for CO₂, H₂S, as well as for the mixture, particularly the molecular mass, heat of vaporization, specific heat and boiling point at 40atm. Several correlations were used as tools in the calculation of these properties.

The heat of vaporization of the individual gases was calculated using the Watson correlation. This correlation, shown in Equation 9, states that is possible to estimate the latent heat of vaporization of a pure liquid at any temperature from the known value at another temperature.

Equation 9: Watson correlation for enthalpy of vaporization

$$\frac{DH_2}{DH_1} = \left(\frac{1 - T_{r2}}{1 - T_{r1}} \right)^{0.38}$$

, where T_r is T/T_{critical} .

Appendix A [87] shows the data utilized for the correlation equations used to obtain the correlations shown in Appendix B. From the data presented in Table 22, the “Add Trendline” Excel function was used to estimate the specific heat at constant pressure of CO₂ at 4MPa. The equation found, with a correlation of $R^2=0.99813$, is shown in Equation 10. In a similar manner, the data presented in Table 23 was used to find a trend line equation to estimate the specific heat at constant pressure of H₂S at 4MPa. The correlation found, with a correlation factor of $R^2=0.99688$, is shown in Equation 11.

Equation 10: Correlation used for CO₂ Specific Heat at constant pressure at 4MPa

$$y = 0.0003x^3 + 0.0375x^2 + 1.5299x + 110.83$$

Equation 11: Correlation used for H₂S Specific Heat at constant pressure at 4MPa

$$y = 0.0017x^2 + 0.1401x + 70.572$$

In a similar manner, the heat capacity at constant pressure was calculated for both CO₂ and H₂S at 2MPa. The data used in this case is shown in Table 24 for CO₂ and in Table 25 for H₂S. By using the same “Add Trendline” function in Excel, two polynomial equations were found to correlate this information. The equations found, shown below as Equation 12 and Equation 13, have a correlation factor of R²=0.99933 and R²=0.99948

Equation 12: Correlation used for CO₂ Specific Heat at constant pressure, 2MPa

$$y = 0.0067x^2 + 0.7642x + 107.76$$

Equation 13: Correlation used for H₂S Specific Heat at constant pressure, 2MPa

$$y = 7E - 6x^3 + 0.002x^2 + 0.1481x + 71.15$$

The same process was followed for estimating the specific heat at constant volume for CO₂ and H₂S at 4MPa. This property is essential in the estimation of power consumption of the compressor, as the power required for compression is directly related to the ratios of specific heats (γ). The equation found for the specific heat at constant volume for CO₂ has a correlation of R²=0.99964 and is shown in Equation 14. The equation found for the specific heat at constant volume for the H₂S has a correlation of R²=99999 and is shown in Equation 15.

Equation 14: Correlation used for CO₂ Specific Heat at constant volume, 4MPa

$$y = 9E - 7x^4 + 0.0001x^3 + 0.0059x^2 + 0.0912x + 41.423$$

Equation 15: Correlation used for H₂S Specific Heat at constant volume, 4MPa

$$y = 0.0003x^2 - 0.0482x + 37.813$$

As before, the heat capacities of CO₂ and H₂S at constant volume were calculated at 2MPa to calculate the corresponding compressor required for the process. The data used for this purpose is shown in Table 24 and Table 25. In this case, the equations

found have a correlation factor of $R^2=0.99989$ and $R^2=0.99991$ for CO_2 and H_2S , respectively, and are shown below as Equation 16 and Equation 17.

Equation 16: Correlation used for CO_2 Specific Heat at constant volume, 2MPa

$$y = 0.0005x^2 - 0.0123x + 40.664$$

Equation 17: Correlation used for H_2S Specific Heat at constant volume, 2MPa

$$y = 0.0004x^2 - 0.0464x + 37.776$$

The estimation of the boiling point of the mixture at 4MPa was performed using the data shown in Table 4 and plotted in Figure 13. The same strategy was following for finding an equation that could correlate the %mol of H_2S in the mixture with the mixtures' boiling point. In this case, the equation found, with a correlation factor of $R^2=0.99998$, is shown in Equation 18.

Equation 18: Correlation used for calculation of mixture boiling point, 4MPa

$$y = 77.344x^4 - 91.010x^3 + 54.954x^2 + 7.9028x + 5.862$$

The boiling point of the mixture at 2MPa was estimated using data shown in table Table 5. Once again, this information was plotted and the Excel's "Add Trendline" function was used to find the best polynomial correlation of the data provided. Unfortunately, very few data points were available for operating pressures of 2MPa, so this correlation is not as exact as the one for an operating pressure of 4MPa. As can be shown in Figure 16, the polynomial equation found for these data points is not as good a fit as the ones shown previously. Nonetheless, the correlation factor is still close to 1, as $R^2=0.99502$.

Equation 19: Correlation used for calculation of mixture boiling point, 2MPa

$$y = 126.14x^3 - 136.72x^2 + 53.434x - 19.08$$

The results of calculating these properties for the feed conditions, for both 4MPa and 2MPa are shown in Table 10. Once the properties for the pure components were found, the properties for the mixture were estimated by using the mol fraction of each component in the mixture. This can be seen intuitively, as the values estimated for the

Table 10: Thermophysical properties calculated for the gas feed

	4MPa			2MPa		
	CO ₂	H ₂ S	Mixture	CO ₂	H ₂ S	Mixture
Molecular Mass (kg/kmol)	44.01	34.08	41.45	44.01	34.08	41.45
Heat of Vap λ (kJ/kmol)	9504.97	11538.33	10030.19	12346.23	14085.04	12795.37
Cp (kJ/kmol-K)	92.83	68.45	86.53	95.16	68.93	88.38
Cv (kJ/kmol-K)	41.30	38.90	40.68	41.11	38.86	40.53
Cp/Cv	2.25	1.76	2.13	2.31	1.77	2.18
Boiling point (°C)	5.86	55.04	10.35	-19.08	23.77	-12.23

mixture resemble closer those of the CO₂ because of its large mol fraction in the feed mixture.

The next step in the preliminary design was to use these properties and the flows resulting from the mass balance (Table 9) to draw the McCabe-Thiele diagram. As explained before, the Rectifying line is drawn from the point (x_D , x_D) to the point (0, $x_D/(R_D+1)$), which, in this case, corresponds to the point (0.974, 0.974) to the point (0, 0.217). The Feedline is drawn from the point (x_F , x_F) upwards with a slope of $(-q/1-q)$, which, in this case, corresponds the point (0.742, 0.742) and a slope of 1.262. Finally, the stripping line is drawn from (x_B , x_B) to the intersection of the Rectifying line and Feed line, which, in this case, corresponds to (0.016, 0.016) to approximately (0.749, 0.799). After drawing the respective “steps” in the diagram, it was found that the ideal number of plates for these particular conditions is 16 plates. The McCabe-Thiele diagram for 40bar operating pressure is shown in Figure 17.

A difference in operating pressure does not have an effect on the slope or points through which the Rectifying and Bottoms line cross. The difference in design comes from a change in the Vapor-Liquid Equilibrium line of the new system and the slope of the feed line. In this case, the feed slope line is 19.623. From this diagram, shown in Figure 18, it is estimated that the number of ideal plates for these particular conditions is 11 plates.

Next, the column diameter calculation procedure followed. This process requires the use of Equation 20, shown below, and Figure 19 shown in Appendix D. This procedure does not calculate the plate spacing within the tower, but leaves this variable free to choose for the design team. For this reason, the results presented in Table 11, show the column radius for different plate spacing.

Equation 20: Correlation required column diameter calculation

$$\frac{L}{V} \left(\frac{r_v}{r_l} \right)^{0.5}$$

Equation 21: Kv value correlation used for column diameter calculation

$$K_v = u_c \left(\frac{r_v}{r_v - r_l} \right)^{0.5} * \left(\frac{20}{S} \right)^{0.2}$$

Using the properties for CO₂ shown in Table 22 and Equation 20, the K_v value for the mixture was estimated at an operating pressure of 4MPa for different tray spacing. From this value, Equation 21 was solved for u_c, which is the vapor velocity within the plates, in feet/s. With this information, the bubbling area of the plates was estimated using the vapor flow vapor speed. As shown in Table 11, the column radius can vary from 2.10cm to 3.43cm for the shortest spacing between plates. Given that this particular project is intended to be only a small laboratory scale, the 3.43cm radius is suggested. This provides the suggested radius calculated by the procedure, but also provides the most flexibility in terms of the total capacity of the distillation tower. If, at any point, during the use of this proposed design the experiment is scaled up from

Table 11: Tray spacing design possibilities for 4MPa conditions

Spacing (in)	$\frac{L}{V} \left(\frac{r_v}{r_l} \right)^{0.5}$	Kv	Column Area (m2)	Column Radius (cm)
36	0.2798	0.32	1.38E-03	2.10
24		0.25	1.77E-03	2.38
18		0.19	2.33E-03	2.72
12		0.16	2.77E-03	2.97
9		0.14	3.16E-03	3.17
6		0.12	3.69E-03	3.43

20kg/h of mixture, a larger diameter column (and hence larger diameter plates) can provide similar fractioning capability without requiring a significantly larger column.

Using the same procedure described in the paragraph above, the K_v value for the mixture was estimated at operating pressure of 2MPa. Once again, Figure 19 was used for estimating the vapor speed through the tower, which in turn was used for calculating the cross-sectional area required inside the column. As shown in Table 12, the column radius varies from 2.03cm for the largest tray spacing to 3.47cm for the shortest tray spacing. These numbers do not vary significantly between operating pressure conditions. This is due to the fact the relationship shown in the x -axis of Figure 19, i.e., Equation 20, is more or less linear in the span corresponding between 0.1757 and 0.2798. This means that, for a change in pressure from 4MPa to 2MPa, the flux of the vapor that is flowing within the tower is not expected to change significantly, and therefore, there is no need for larger diameter column to accommodate the different flow rate of vapor.

Theoretically, the tray spacing could be smaller than the smallest spacing suggested by Figure 19. However, estimating K_v can be unreliable for separations below 6 inches (15.2cm) as data is not provided by the correlations used in that figure. As can be seen from Figure 19, the K_v value is directly proportional to the vapor speed, which in turn is directly proportional to the tray spacing. Even though no direct correlation is provided for tray spacing below 6 inches, it is reasonable to expect slower vapor speeds within the tower if it were constructed with shorter spacings. This would mean a slightly wider and shorter distillation column.

Although there have been studies made regarding plate efficiency, the estimation

Table 12: Tray spacing design possibilities for 2MPa conditions

Spacing (in)	$\frac{L}{V} \left(\frac{r_v}{r_l} \right)^{0.5}$	K_v	Column Area (m ²)	Column Radius (cm)
36	0.1757	0.38	1.30E-03	2.03
24		0.3	1.64E-03	2.29
18		0.22	2.24E-03	2.67
12		0.18	2.74E-03	2.95
9		0.15	3.28E-03	3.23
6		0.13	3.79E-03	3.47

of efficiency is largely empirical, but there is sufficient data at hand to show what are the major factors involved in higher or lower efficiencies. At the same time, plate efficiency is strongly dependent on the rate of mass transfer between liquid and vapor. This means that adequate contact between vapor and liquid is essential and any problems in operation, such as excessive foaming or entrainment or poor vapor distribution can lower the plate efficiency.

High plate efficiencies are normally associated with a high Peclet number. This number correlates the length of liquid flow path with the eddy diffusivity and residence time of the liquid on the plate, as shown in Equation 22, shown below. Moreover, columns operated at high velocity will have significant entrainment. This means that the drops of entrained liquids are less rich in the more volatile component than that in the vapor, which translates into reduced plate efficiency.

Equation 22: Peclet number

$$N_{Pe} = \frac{Z_t^2}{D_e t_L}$$

As can be seen from Figure 19, the vapor velocity is directly proportional to the K_v value and they are inversely proportional to the column radius. Therefore, overall, plate efficiency is directly proportional to the radius of the tower and inversely proportional to the vapor speed. This means that a low vapor speed translates to better plate efficiency, concurring well with the short analysis discussed previously regarding columns operating with high entrainment.

Unfortunately, for this project, there is no theoretical basis for calculating, or estimating neither the plate nor overall efficiency of the column. However, a conservative 80% efficiency was assumed. This would give this tower a total of 20 plates for an operating pressure of 4MPa and 14 plates for an operating pressure of 2MPa. With the proposed 6in separation between plates, the tower would be approximately 3.05m tall for the high operating pressure and 2.15m tall for the low operating pressure.. These characteristics are summarized in Table 13.

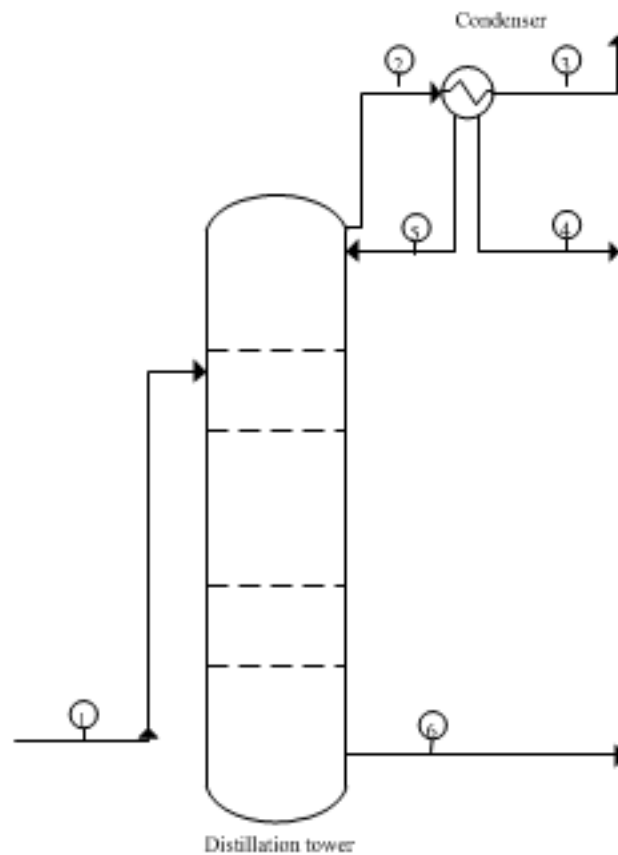
The process flow diagram of the distillation process, shown in Figure 9, labels different streams from stream 1 to stream 6. As shown there, stream 1 represents the overall mixture entering the column, which is distilled and labeled as stream 2. After going through the condenser, this stream is separated into stream 3, which would

Table 13: Distillation tower characteristics

	Pressure of 4MPa	Pressure of 2MPa
Theoretical plates	16	11
Real plates	20	14
Plate separation (in/cm)	6/15.2	
Tower diameter (cm)	6.86	6.94
Tower height (m)	3.05	2.15
Material of construction	Stainless Steel 316-L	

provide gaseous CO₂, stream 4, which would provide liquid CO₂ and stream 5, which is the fraction of distillate that is returned to the distillation tower in the form of reflux. Finally, the bottoms stream, which contains the stream rich in H₂S, is labeled as stream 6. Table 14 shows the calculated flows for each stream, serving as the overall mass balance for the system.

The system design began on the basis of what a typical distillation column consists of. The minimum equipment required for this laboratory scale project would

**Figure 9: Process flow diagram of proposed system**

be a compressor, one condenser on the distillate flow, one level transmitter, one pressure transmitter, six control valves and one Programmable Logic Controller (PLC).

The process begins with an inlet gas flow that reaches a flow meter and the first control valve, labeled FT-1 and V-1 in Figure 10, respectively. This flow transmitter will calculate the gas flow rate in the pipe and send the information to the PLC (solid blue line, same figure), which will instruct the flow control valve, V-1 (dashed blue line, same figure), to open or close in such a way that the 20kg/h flow rate is achieved. The specifications for the flow transmitter FT-1, shown in Table 15 include an operating temperature range of -40°C to 200°C, comfortably able to operate successfully under the proposed distillation procedure. The transmitter is a “clamp” type transmitter, meaning that it’s independent of the size of the pipe it will be connected to. This transmitter is an ultrasonic transmitter, which means it measures the flow rate indirectly and so is also independent of the pressure conditions of the gas and it also does not require a particular construction material, as it is not exposed to the corrosive effects of H₂S. The connection available for the transmitter is an RS-232

Table 14: Distillation process mass balance

Stream	Composition	%mol	Flow (kmol/h)	Pressure (MPa)	Temperature (°C)
1	CO ₂	74.2	0.3579	4	-20
	H ₂ S	25.8	0.1246		
2	CO ₂	97.4	0.3561	4	-20
	H ₂ S	2.6	0.0094		
3	CO ₂	97.4	0.2770	4	-20
	H ₂ S	2.6	0.0073		
4	CO ₂	97.4	-	4	-20
	H ₂ S	2.6	-		
5	CO ₂	97.4	0.0791	4	-20
	H ₂ S	2.6	0.0021		
6	CO ₂	1.6	0.0018	4	-20
	H ₂ S	98.4	0.1153		
Condenser			13.89		

Table 15: Specifications for flow transmitter FT-1

	Description
Size	Independent of pipe size
Operating temperature range	-40°C to 200°C
Operating pressure range	Independent of pressure conditions
Connection	RS-232
Transmitter output	4-20mA

cable with an output of 4-20mA.

On the other hand, valve V-1 is in direct contact with the gas mixture, so it has different specifications regarding construction material. This valve would need to be built of stainless steel 316-L to be able to withstand the corrosive effects of the gas mixture. Its connection to process is NPS ½ and the valve has a flow factor of 0.25 at 60% opening, according to the manufacturer. The valve is certified to operate between -195°C to 93.3°C and up to 178 bar, comfortably handling the operating conditions of the system. These specifications are summarized in Table 16.

Next, the flow will reach valves V-2 and V-3, shown in Figure 10. The purpose of these valves would be for purely safety reasons. These valves would be normally open (N/O) and close in the event of unexpected operational circumstances. Again, these valves would be in contact with the corrosive mixture and so would require a stainless steel 316-L construction. The valves chosen would have the same characteristics as valve V-1, as shown in Table 16.

The distillation tower will have a level transmitter connected at the bottom of the tower, shown as LT-1 in Figure 10. This transmitter would send the level readings to the PLC (solid green line in same figure), which would control valve V-6, also shown in the same Figure. The purpose of this instrumentation loop is to balance the possible changes in liquid level, minimizing the fluctuations that could interfere with the optimum operation of the distillation column. The level transmitter selected is a coplanar, gage pressure type. Since it is in direct contact with the mixture, it would be constructed of stainless steel 316-L. The process connection is ¼ 18NPT and would be able to operate at pressures between -0.98 bar to 137.9 bar. The output of the transmitter is also 4-20mA. These specifications are summarized in Table 17.

The valve to which this loop would be connected, V-6 would also be in direct contact to H_2S . The valve for this point in the process would have the same characteristics as those of valves V-2 and V-3 previously discussed.

A pressure transmitter would be installed at the top of the distillation tower. This transmitter, labeled PT-1 in Figure 10, would be connected to the PLC (solid red line, same figure), which would instruct valve V-4 (dashed red line, same figure) to open or close in a manner that the 40bar operating pressure is maintained within the distillation tower. This pressure transmitter is also a coplanar gauge pressure type, with a body made of carbon steel but an isolating diaphragm made of stainless steel

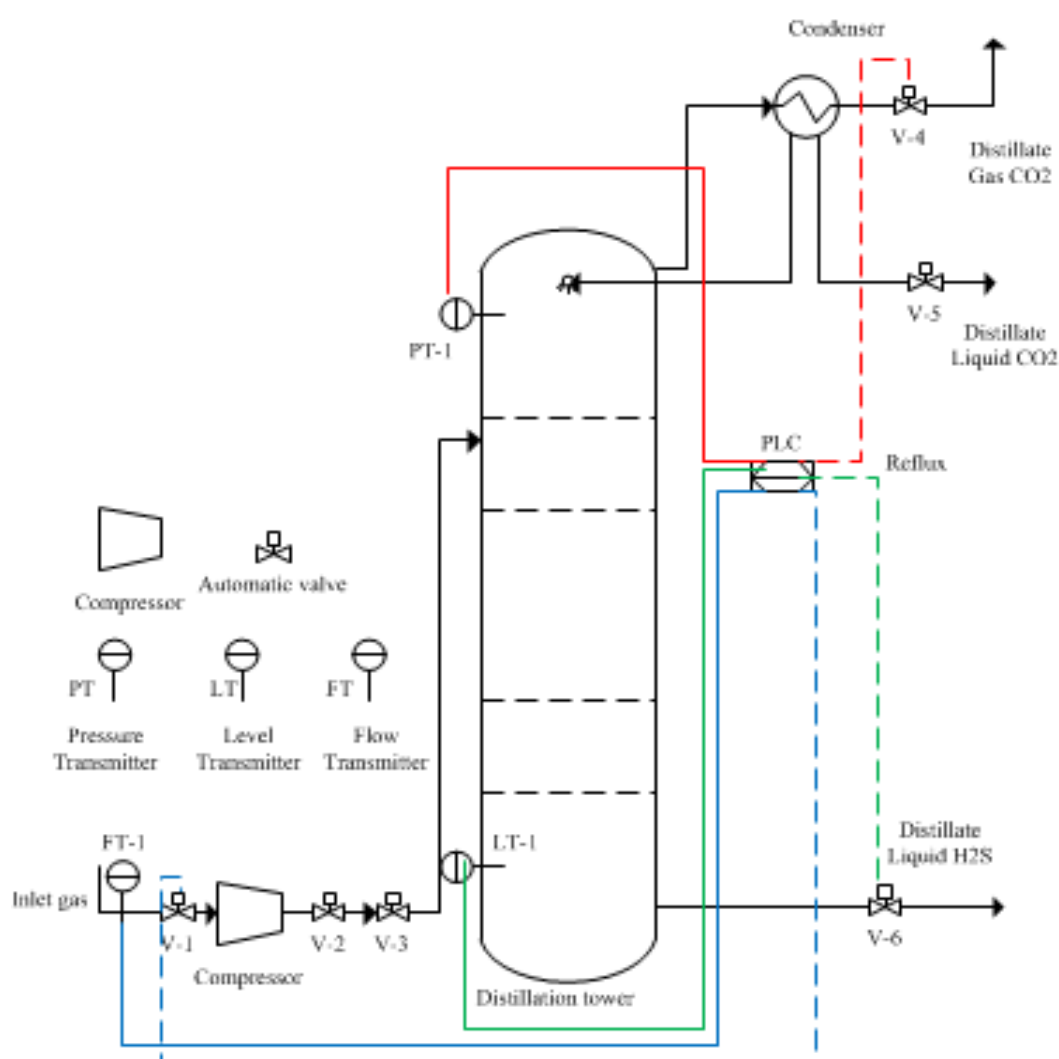


Figure 10: Piping and Instrumentation Diagram of the proposed system

Table 16: Specifications for automatic valves V-1, V-2, V-3 and V-6

	Description
Material of construction	Stainless steel 316-L
Process connection	NPS 1/2
Flow factor	0.25 at 60% opening
Operating temperature range	-195°C to 93.3°C
Operating pressure range	Up to 178 bar.

316-L to be able to withstand the he corrosive conditions inside the distillation tower. Its process connection would be a flange ¼ 18NPT. According to the manufacturer, this transmitter would be able to operate between -0.98 bar to 137.9 bar and its transmitter output is 4-20mA. These characteristics are summarized in Table 18

Valve V-4, which would be the valve connected to this instrumentation loop, would only be in contact with CO₂, a chemical far less corrosive than H₂S. For this reason, this valve can be constructed of carbon steel. Its process connection would be also a flange ¼ 18NPT and would have a transmitter output of 4-20mA. These characteristics are summarized in Table 19

The distillation tower would also be fitted with valve V-5, shown in Figure 10, whose purpose would be to allow the flow of liquid CO₂ out from the tower. As with valve V-4, this valve would only be in contact with CO₂ and so strict materials of construction would not be needed. For this purpose, it was decided that this valve have the same specifications as valve V-4. As described before, these specifications are summarized in Table 19.

The final electronic device in this design would be the Programmable Logic Controller, PLC, which would be in charge of interpreting the signals incoming from

Table 17: Specifications for level transmitter LT-1

	Description
Type	Coplanar, gauge pressure
Material of construction	Stainless steel 316-L
Process connection	DIN ¼ 18 NPT 316-L stainless steel
Operating pressure limit	-0.98 bar to 137.9 bar
Transmitter output	4-20mA

the different sensors. As can be seen from Figure 10, the PLC would require having at least 3 inputs and being able to provide 3 output connections. For this reason, the chosen PLC, as shown in Table 20, has 6 digital entries and 4 digital outputs, which would allow a connection of all the instruments proposed for this system and still have spare connections for any extra instruments that could be required. This PLC also has the advantage of being expandable, meaning it would be possible to connect new entry and exit modules if it would be required to expand its capacity.

A simple energy balance at the top of the tower shows that, for the estimated flow of distillate, the condenser would need to remove approximately 15,634 kJ/h. Assuming cooling water is used in the condenser to remove this heat, and assuming a temperature rise of 15K for this water, the system would require approximately 249.92kg/h of water, or 13.89 kmol/h, as shown in the overall mass balance in Table 14. This condenser would be required to be a surface condenser because it is not advisable to return liquid water to the distillation tower as the conditions may favor the formation of gas hydrates.

An analogous energy balance for the tower operating at 2MPa shows that the condenser would need to remove approximately 20,309kJ/h. Assuming the same temperature drop for these conditions, the system would require approximately 324.63kg/h of water, or 18.01kmol/h.

The compression ratio for this process is approximately 41. For a multistage compressor, it can be shown that the total power is a minimum if each stage does the same amount of work. In this case, the total power required by the compressor would be the power required by each stage, times the number of total stages. Given the compression ratio, this process would be best suited for a three-stage compressor, and, therefore, the compression ratio of one stage should be the cube root of the overall

Table 18: Specifications for pressure transmitter PT-1

	Description
Type	Coplanar, gauge pressure
Material of construction	Carbon steel
Isolating diaphragm	Stainless steel 316-L
Process connection	Flange, ¼ 18NPT
Operating pressure limit	-0.98 bar to 137.9 bar
Transmitter output	4-20 mA

compression ration. The calculation of the power required is a function of the ratio between specific heat at constant pressure and at constant volume. For this calculation, the dimensional equation utilized was Equation 23, where T_a is the inlet temperature, in K, γ is the C_p/C_v ratio, η is the efficiency of the compressor, q_0 is the volumetric flow of the compressed gas, (m^3/s), p_B and p_a are the discharge and inlet pressures, respectively.

Equation 23: Power required by a compressor

$$P_B = \frac{0.371T_a g q_0}{(g - 1)h} \left[\left(\frac{p_B}{p_A} \right)^{1-\frac{1}{g}} - 1 \right]$$

By using the heat capacity at constant pressure and the heat capacity at constant volume, shown in Table 10, it was found that the power required for the compressor is approximately 3.06kW when working at 4MPa and 2.37kW when working at 2MPa.

A simple analysis of these water and electricity requirements shows that, for the 4MPa operating pressure, it is needed approximately 20.50 kg of cooling water per kg of CO₂ separated and approximately 0.293kW of compressor load per kg of CO₂ separated. On the other hand, for the 2MPa operating pressure, it is needed approximately 26.63 kg of cooling water per kg of CO₂ separated and approximately 0.226kW of compressor load per kg of CO₂ separated. This translates to a 29.9% more cooling water required for lower operating pressure, but approximately 22.7% less compressor load per kg of CO₂ separated. This information is tabulated in Table 21

It is immediately intuitive why there is a reduction in the compressor load per kg of gas distilled, as for a lower operating pressure is it required less work by a compressor to reach said operating conditions. Despite the pressure going down in half, the load is not lowered in half because the power required by the compressor is

Table 19: Specifications for automatic valves V-4 and V-5

	Description
Material of construction	Carbon steel
Process connection	Flange ¼ 18NPT
Size	½ inch (1.27cm)
Transmitter output	4-20 mA

not a linear function of the compression ratio required of the equipment, but rather a complicated equation exponentially dependent on the C_p/C_v ratio.

On the other hand, it may not be immediately intuitive why more cooling water is necessary when the operating conditions are not as severe. At higher temperatures, the vapor pressure of liquids is higher. Therefore, the system would require less energy input to reach a point where the vapor pressure equals the pressure of the surroundings, or the definition of boiling. Since the heat of condensation is equal to the heat of vaporization with a negative sign, it can be said that at higher temperatures, it's necessary to remove less energy from the system in order for the gas to condense. In other words, the so that its particles interact more with one another. The reduction in thermal energy supplied leads to a reduction in the speed at which the particles move. This reduced momentum may also lead to a higher degree of gas particle interaction, and a higher degree of non-covalent interaction, which causes the gas as a whole to reduce in volume as the particles are drawn closer to each other.

Inversely, for a lower boiling point system, more energy removed is required because it's necessary to bring the vapor pressure of the gas even lower in order for it to condense. This means that, for the same temperature rise of cooling water, more water is required.

Since the process of condensation is simply the removal of enough energy in the gaseous phase of a compound the case of this distillation system, the choice of optimal operating pressure is a trade-off between less water consumed in the condenser (and therefore lower pump requirements) or less duty required by the gas compressor. This decision cannot be made using this laboratory scale experimental proposed setup because a full-size plant could have very different performance parameters. In other words, equipment performance and efficiency, or general system

Table 20: Specifications for Programmable Logic Controller

	Description
Digital entries / analog entries	6/0
Digital outputs / analog outputs	4/0
Connections	RS-232
Other	Adaptable to Ethernet / IP connection

Table 21: Utilities required per kg of NCG

Requirement	4MPa	2MPa	Difference (%)
Cooling water (kg/kg NCG initial flow)	12.496	16.231	29.9%
Cooling water (kg/kg CO ₂ distilled)	20.503	26.632	
Compressor load (kW/kg NCG initial flow)	0.178	0.138	-22.7%
Compressor load (kW/kg CO ₂ distilled)	2.93E-1	2.26E-1	

operating behavior, may not be linear, and certainly equipment cost will not be linear (particularly pump capital and operating costs and compressor capital and operating costs). However, it is useful to know these performance parameters (kg of cooling water per kg of distilled NCG and compressor kW duty per kg of NCG) and how they behave under different operating conditions beforehand in order to minimize unpleasant surprises when the planning, construction and operation of a full size facility comes to be.

Overall, it is recommended that this laboratory scale tower be built using modular design. This

means to design and build the different components of the system separately and test each component in separate conditions. Using this approach, the system can be subdivided into smaller parts that can be independently created and then used in different system to drive multiple functionalities. This way, each system is partitioned into discrete, scalable, reusable modules, consisting of isolated, self-contained functional elements. In this manner, the construction cost of the final system is reduced at the same time the flexibility of the design is increased. Modularity also offers other benefits, such as augmentation and exclusion (adding or removing pieces by merely plugging in a new module). This way, different materials can be tested at different operating conditions and the overall performance of the distillation tower can be evaluated. In other words, this design approach allows different aspects of the design to be worked on and improved independently of each other, thereby optimizing the performance of the system in a way that a conventional design may not.

The benefits of a modular design approach can be even greater if it is used across an entire production system, not just one equipment. Any product or system could potentially be modularized, but it is necessary to be selective in choosing which equipment to design, or redesign, with this approach. To more easily benefit from the advantages of modular design, it is best to target equipment that have a large number

of shared components with other systems, such as condensers, compressors, demisters, instrumentation, etc.

In a general sense, a team comprised of overly specialized individuals can inhibit the ability of the team to look across equipment and systems to separate modular components. Companies should establish “modular design teams” that possess a broader technical skill set, as well as acute insight into the procurement processes to understand and explore the full range of modular design possibilities that exist across a power plant.

7. Conclusions

7.1. Conclusions for H₂S abatement methods

Many H₂S abatement processes have been developed over the past decades. Selecting an appropriate abatement method requires analyzing several variables, such as geothermal brine characteristics, abatement efficiency, process economics, and geothermal plant design, among others. Thus, the process of selecting an abatement method can be complicated. The present work explored some of the most widely used H₂S abatement methods in the industry and provided a preliminary assessment on the basis of available qualitative criteria. Evidently, more detailed, quantitative assessment procedures are needed for particular cases for selecting the most appropriate abatement method. This paper, however, attempts to serve as a preliminary decision tool for selecting abatement systems. By using the criteria described in Table 6, some processes, or combination of processes are proposed. All of the proposed methods are considered effective, achieving over 90% removal of H₂S entering the geothermal fluid.

The key variables identified during the literature research are the following:

- The economics of the process. Some abatement methods are more complex than others, and so the capital costs and operating costs can vary widely among them. The more complex systems usually require high capital investment but can have low operating costs. Meanwhile, the more simple processes usually require low capital costs but are subject to high operating costs.
- The ratio of ammonia-to-hydrogen sulfide in the geothermal brine, as the pH of the brine is key to the type and rate of reaction that can take place along the abatement process.
- Condenser design. The chemical reactions taking place among different processes can require a different type of condenser in the power plant.

The methods that presented the most advantages included scrubbing with alkali, liquid redox methods, reinjection of NCG, Selectox, Dow-Spec RT-2 and BIOX.

In general, scrubbing with alkali, reinjection of NCG and the BIOX process appear to have some economic advantages in that their demand for capital investment is lower than other methods. In general, methods such as these that require low capital

investment but have relatively high operating costs may be suitable for smaller units, of relatively short lifetime. On the other hand, processes such as Selectox or the Dow-Spec RT-2 are more suitable for large units, which can take on additional capital costs but undergo low operating costs throughout the lifetime of the geothermal plant.

Adoption of any process must also take into consideration the content of ammonia in the geothermal brine. For example: the liquid redox, NCG reinjection, Selectox, stream stripping and Dow-Spec RT-2 processes require a low concentration of ammonia in the geothermal brine. On the other hand, the H_2O_2 is best suited for high ammonia content. The scrubbing with alkali and the BIOX processes present the most flexibility regarding this variable, as they can be adapted and used in geothermal fields with high and low concentration of ammonia.

As mentioned before, this work only aims to provide simple guidelines and to point out the key variables identified during the literature research in this topic. This relatively small group of processes must be subject to a more detailed, quantitative technical and economical assessment for final selection of the optimum process, or combination of processes.

7.2. Conclusions for proposed distillation process

Although many H_2S abatement methods are available and used in different geothermal plants across the world, few, if any, were economically feasible for Reykjavík Energy to operate in Iceland. However, it appears that using distillation as a method of abating H_2S emissions is potentially possible and perhaps economically beneficial in the particular context of Iceland. Theoretically, different levels of CO_2 purity can be achieved through this method, but special analysis should be made to determine the economical optimum purity of gas output.

The design process lead to a distillation system with relatively little equipment required but with a relatively complex operation. It must be clarified that the complexity of the operation does not lie in the distillation procedure on itself, but rather in preventing the formation of hydrates. As has been discussed in the background information of this work, there are several methods available for preventing the formation of hydrates, some that would require more intensive capital or operational expenses. These systems, nonetheless, should be adapted to use in the geothermal industry, from experience in the oil and gas industry.

At the same time, special care must be placed in material selection. The gas mixture, which the system is meant to separate, contains a significant percentage of H_2S , a highly corrosive gas. For this reason, not all materials are suited for this application. The material selection ought to reflect the overall philosophy regarding design life, cost, maintenance, safety and environmental concerns. A detailed material selection process should take into account specified operating conditions, including start up and shutdown conditions. Particularly important is also to study the failure probabilities and consequences to human health, environment and assets. Assuring that the design allows for access for maintenance and repair is also important in the design phase.

From the results presented by the SulFix project carried out at Reykjavík Energy, it appears that it is possible to reinject the H_2S separated back to the geothermal reservoir without significant operational drawbacks. Simulations performed by [52] predict efficient precipitation of H_2S into thermodynamically stable minerals. This means that the reinjection of H_2S back underground, under Icelandic geological and thermal conditions, should not encounter the problems reported at the Coso geothermal field.

More research should be performed in order to decide whether or not reinjecting H_2S is the best way of disposing of this gas. Hydrogen sulfide does have a relatively high heat of combustion, meaning it could be possible to burn the gas and, through a heat exchanger, produce steam that could increase the power output of the power plant. This method is applied in certain geothermal facilities but has limited application, as the flow of H_2S can be intermittent and produce an erratic flame. However, the hydrogen sulfide content in the Hengill area is generally considered to be high, so these types of problems could be minimized.

A few performance parameters were calculated with this experimental setup, namely the amount of cooling water required and compressor load required per kg of NCG in the initial flow and the kg of CO_2 distilled. This simple analysis, done at two different operating pressure, show that the cooling water needed for operation is inversely proportional to the operating pressure, while the compressor load is directly proportional. For the conditions estimated, there is approximately a 30% increase in the cooling water required when operating this tower at half the pressure that it was initially operated at during Reykjavík Energy's pilot tests. On the other hand, there

was nearly a 23% decrease in the required power needed in the compressor for the same operating pressure difference. These numbers should only serve as guidelines and should not be scaled up linearly to a full-size separation plant, as performance of equipment and efficiencies could change dramatically with a significant change in the flow of gas treated.

A more detailed chemical separation performance evaluation should be performed in order to estimate with more certainty how this system would behave when treating large amounts of gas. Simulation is a powerful tool for estimating and optimizing results. Through this way, it is possible to understand better the behavior of the system along several years of operation, particularly regarding efficiency of equipment, corrosion of pipelines, probability of forming hydrates, etc. With a basic spreadsheet tool, it would be possible to attain good solutions without having to purchase expensive simulation software.

8. References

- [1] United Nations Environment Programme, World Meteorological Organization, Intergovernmental Panel on Climate Change, and Potsdam-Institut für Klimafolgenforschung, *Renewable energy sources and climate change mitigation: special report of the Intergovernmental Panel on Climate Change*. New York: Cambridge University Press, 2012.
- [2] “Primary energy use | Primary Energy | Energy Statistics | Energy Data | Orkustofnun | National Energy Authority of Iceland.” [Online]. Available: <http://www.nea.is/the-national-energy-authority/energy-statistics/primary-energy/>. [Accessed: 01-Oct-2013].
- [3] A. Holm, D. Jennejohn, and L. Blodgett, “Geothermal Energy and Greenhouse Gas Emissions,” Geothermal Energy Association, Nov. 2012.
- [4] Massachusetts Institute of Technology, *The future of geothermal energy: impact of enhanced geothermal systems (EGS) on the United States in the 21st century: an assessment*. Cambridge, Mass.: Massachusetts Institute of Technology, 2006.
- [5] B. M. Júlíusson, “Reducing H₂S Emissions from Geothermal Power Plants. Collaboration of Icelandic Energy Companies,” presented at the From Waste to Value, GEORGE seminar, Reykjavik, Apr-2013.
- [6] European Environment Agency, “Air Pollution (Iceland),” *Air Pollution*, May-2013. [Online]. Available: http://www.eea.europa.eu/soer/countries/is/soertopic_view?topic=air%20pollution. [Accessed: 31-May-2013].
- [7] M. S. Legator, C. R. Singleton, D. L. Morris, and D. L. Philips, “Health Effects from Chronic Low-Level Exposure to Hydrogen Sulfide,” *Arch. Environ. Health*, vol. 56, no. 2, p. 123, Mar. 2001.
- [8] Icelandic Environmental Agency, “Brennisteinsvetni,” *Umhverfisstofnun*, 2013. [Online]. Available: <http://www.ust.is/einstaklingar/loftgaedi/brennisteinsvetni/>. [Accessed: 31-May-2013].
- [9] W. Duffield and J. Sass, “Geothermal Energy - Clean Power from the Earth’s Heat.” U.S. Geological Survey, Mar-2003.

- [10] R. DiPippo, *Geothermal power plants principles, applications, case studies and environmental impact*. Amsterdam; Boston; London: Butterworth-Heinemann, 2008.
- [11] William Scott Harvey, Sep-2013.
- [12] A. Kagel, D. Bates, and K. Gawell, "A Guide to Geothermal Energy and the Environment," Geothermal Energy Association, Apr. 2007.
- [13] R. J. Reiffenstein, W. C. Hulbert, and S. H. Roth, "Toxicology of Hydrogen Sulfide," *Annu. Rev. Pharmacol. Toxicol.*, vol. 32, no. 1, pp. 109–134, 1992.
- [14] WHO Regional Office for Europe, "Chapter 6.6 - Hydrogen Sulfide," in *Air Quality Guidelines*, Second., Copenhagen, Denmark: WHO, 2000.
- [15] "Renewable Energy Sources and Climate Change Mitigation," Intergovernmental Panel on Climate Change, 2012.
- [16] Ministry for the Environment, "Ambient Air Quality Guidelines - 2002 Update," Ministry for the Environment, Wellington, New Zealand, 32, May 2002.
- [17] California Environmental Protection Agency, "History of Hydrogen Sulfide Ambient Air Quality Standard." [Online]. Available: <http://www.arb.ca.gov/research/aaqs/caaqs/h2s/h2s.htm>. [Accessed: 29-Sep-2013].
- [18] Bay Area Air Quality Management District, "Regulation 9: Inorganic Gaseous Pollutants. Rule 5: Hydrogen Sulfide from Geothermal Power Plants," Bay Area Air Quality Management District, Mar. 1982.
- [19] A. Khaghani, A. Date, and A. Akbarzadeh, "Sustainable removal of non-condensable gases from geothermal waters," *Renew. Sustain. Energy Rev.*, vol. 21, pp. 204–214, May 2013.
- [20] N. Y. Ozcan and G. Gokcen, "Thermodynamic assessment of gas removal systems for single-flash geothermal power plants," *Appl. Therm. Eng.*, vol. 29, no. 14–15, pp. 3246–3253, Oct. 2009.
- [21] R. B. Chaves, "Geothermal gases as a source of commercial CO₂, in Miravalles, Costa Rica and Haedarendi, Iceland," United Nations University, Reykjavik, Iceland, 3, 1996.
- [22] A. Stefánsson, S. Arnórsson, I. Gunnarsson, H. Kaasalainen, and E. Gunnlaugsson, "The geochemistry and sequestration of H₂S into the geothermal

- system at Hellisheidi, Iceland,” *J. Volcanol. Geotherm. Res.*, vol. 202, no. 3–4, pp. 179–188, May 2011.
- [23] H. E. Khalifa and E. Michaelides, “Effect of non condensable gases on the performance of geothermal steam power systems,” Brown Univ., Providence, RI (USA). Dept. of Engineering, COO-4051-36, Nov. 1978.
- [24] R. Ojala, “Keep Ejectors Online,” May-1992. [Online]. Available: http://www.che.com/articles/1985-1999/Vol99/chevol99_num5_28.html. [Accessed: 29-May-2013].
- [25] S. Walas, *Chemical Process Equipment. Selection and Design*. Reed Publishing, 1990.
- [26] E. E. Ludwig, *Applied process design for chemical and petrochemical plants*, 3rd ed. Houston: Gulf Pub. Co, 1995.
- [27] K. Torzewski, “Facts at your Fingertips: Vacuum Pumps,” Jul-2008. [Online]. Available: http://www.che.com/technical_and_practical/4005.html. [Accessed: 29-May-2013].
- [28] M. Forsha, K. Nichols, and J. Shull, “Development and Operation of a Turbocompressor for non-condensable Gas Removal at Geothermal Power Plants,” *Geotherm. Resour. Counc. Trans.*, vol. 23, pp. 59–63, Oct. 1999.
- [29] M. Forsha and K. Lankford, “Turbine-driven compressors for noncondensable gas removal at geothermal steam power plants,” in *INTERSOCIETY ENERGY CONVERSION ENGINEERING CONFERENCE*, 1994, vol. 4, pp. 1620–1620.
- [30] H. Hamano, “Design of a Geothermal Power Plant with High Non-condensable gas content,” *Geotherm. Resour. Counc. Trans.*, vol. 7, pp. 15–18, Oct. 1983.
- [31] M. Vorum and E. Fritzler, “Comparative Analysis of Alternative Means for Removing Noncondensable Gases from Flashed-Steam Geothermal Power Plants,” National Renewable Energy Laboratory, Jun. 2000.
- [32] R. B. Swandaru, “Thermodynamic analysis of preliminary design of power plant unit I Patuha, West Java, Indonesia,” United Nations University, 2006.
- [33] V. Bontozoglou and A. J. Karabelas, “Direct-contact steam condensation with simultaneous noncondensable gas absorption,” *AIChE J.*, vol. 41, no. 2, pp. 241–250, 1995.

- [34] D. Sanopoulos and A. Karabelas, "H₂S Abatement in Geothermal Plants: Evaluation of Process Alternatives," *Energy Sources*, vol. 19, no. 1, pp. 63–77, 1997.
- [35] G. G. Gunerhan and G. Coury, "Upstream reboiler design and testing for removal of non-condensable gases from geothermal steam at Kizildere Geothermal Power Plant, Turkey," in *Proceedings World Geothermal Congress*, Japan, 2000, pp. 3173–3178.
- [36] F. Stephens, J. Hil, and P. J. Phelps, "State-Of-The-Art Hydrogen Sulfide Control for Geothermal Energy Systems," U.S. Department of Energy, Mar. 1980.
- [37] H. ter Maat, J. A. Hogendoorn, and G. F. Versteeg, "The removal of hydrogen sulfide from gas streams using an aqueous metal sulfate absorbent: Part I. The absorption of hydrogen sulfide in metal sulfate solutions," *Sep. Purif. Technol.*, vol. 43, no. 3, pp. 183–197, Jun. 2005.
- [38] L. Owen and D. Michels, "Geochemical Engineering Reference Manual," U.S. Department of Energy, Jan. 1984.
- [39] D. Mamrosh, K. McIntush, C. Beitler, S. Markússon, and K. Einarsson, "Screening of H₂S Abatement Options for Geothermal Power Noncondensable Gas at Bjarnarflag," *GRC Trans.*, vol. 36, pp. 1217–1226, 2012.
- [40] J. Farison, B. Benn, and B. Berndt, "Geysers power plant H₂S abatement update," in *Geoth*, 2010, vol. 34, pp. 1229–1234.
- [41] D. A. Dalrymple, T. W. Trofe, and J. M. Evans, "Liquid redox sulfur recovery options, costs, and environmental considerations," *Environ. Prog.*, vol. 8, no. 4, pp. 217–222, 1989.
- [42] H. W. Gowdy, D. D. Delaney, and D. M. Fenton, "Vanadium Catalyzed Autoxidation of Hydrogen Sulfide," in *Oxygen Complexes and Oxygen Activation by Transition Metals*, A. E. Martell and D. T. Sawyer, Eds. Springer US, 1988, pp. 203–213.
- [43] H. K. Abdel-Aal, *Petroleum and gas field processing*. New York: Marcel Dekker, 2003.
- [44] World Environment Center, "Technical assessment on H₂S gas abatement systems at California Energy's Coso Geothermal Power Plants," US-Asia Environmental Partnership.

- [45] R. A. Pandey and S. Malhotra, "Desulfurization of gaseous fuels with recovery of elemental sulfur: An overview," *Crit. Rev. Environ. Sci. Technol.*, vol. 29, no. 3, p. 229, 1999.
- [46] R. A. Douglas, "Hydrogen sulfide oxidation by naphthoquinone complexes the hiperion process," *Am Chem Soc Div Fuel Chem*, vol. 35, pp. 136–149, 1990.
- [47] G. Nagl, "Coso Geothermal Field - 15 years of successful H₂S emission abatement." Dec-2009.
- [48] Merichem Company, "LO-CAT II Process. Control H₂S Emissions at Geothermal Plants."
- [49] A. Baldacci, "AMIS: An Innovative Technology for Hydrogen Sulfide and Mercury Abatement from Geothermal Gases," *Geothermal*, vol. 28, pp. 511–514, Sep. 2004.
- [50] A. Baldacci, M. Mannari, and F. Sansone, "Greening of geothermal power: an innovative technology for abatement of hydrogen sulphide and mercury emission," in *Proceedings World Geothermal Congress, Antalya, Turkey*, 2005.
- [51] R. Bonciani, A. Lenzi, F. Luperini, and F. Sabatelli, "Geothermal power plants in Italy: increasing the environmental compliance," presented at the European Geothermal Conference, Italy, 2013, pp. 1–5.
- [52] Edda S.P. Aradóttir, Ingvi Gunnarsson, Bergur Sigfússon, Gunnar Gunnarsson, Einar Gunnlaugsson, Hólmfríður Sigurðardóttir, Einar Jón Ásbjörnsson, and Eric Sonnenthal, "Towards Cleaner Geothermal Energy Utilization: Capturing and Sequestering CO₂ and H₂S Emissions from Geothermal Power Plants," in *TOUGH Symposium 2012*, Lawrence Berkeley National Laboratory, Berkeley, California, 2012, p. 8.
- [53] C. Vancini, "Peabody-Xertic, A New Process to Desulfurize Geothermal Non-condensable Gas Streams," *Geotherm. Resour. Counc. Trans.*, vol. 10, pp. 293–298, Sep. 1986.
- [54] K. V. Matthíasdóttir, "Removal of Hydrogen Sulfide from Non-Condensable Geothermal Gas at Nesjavellir Power Plant," Department of Chemical Engineering, Lund Instituted of Technology, Lund, Sweden, Jun. 2006.
- [55] K. Takahashi and M. Kuragaki, "Yanaizu-Nishiyama Geothermal Power Station H₂S Abatement System," presented at the World Geothermal Congress, 2010.

- [56] A. Benschop, A. Janssen, A. Hoksberg, M. Seriwala, R. Abry, and C. Ngai, "The Shell-Paques/THIOPAQ Gas Desulfurization Process: Successful Startup First Commercial Unit."
- [57] P. Mandalaparti, M. Deo, J. Moore, and B. McPherson, "Carbon dioxide sequestration: Effect of the presence of sulfur dioxide on the mineralogical reactions and on the injectivity of CO₂+ SO₂ mixtures," *Univ. Utah Salt Lake City*, 2009.
- [58] E. Y. Li, D. A. Chareev, S. N. Shilobreeva, D. V. Grichuk, and O. A. Tyutyunnik, "Experimental study of sulfur dioxide interaction with silicates and aluminosilicates at temperatures of 650 and 850°C," *Geochem. Int.*, vol. 48, no. 10, pp. 1039–1046, Oct. 2010.
- [59] B. R. Ellis, L. E. Crandell, and C. A. Peters, "Limitations for brine acidification due to SO₂ co-injection in geologic carbon sequestration," *Int. J. Greenh. Gas Control*, vol. 4, no. 3, pp. 575–582, May 2010.
- [60] L. Andre, M. Azaroual, C. Bernstone, and A. Wittek, "Modeling the Geochemical Impact of an Injection of CO₂ and Associated Reactive Impurities into a Saline Reservoir," in *PROCEEDINGS, TOUGH Symposium 2012*, Berkeley, États-Unis, 2012, p. 8 p.
- [61] RMT Inc., "Calpine enhanced geothermal systems project. Final environmental assessment.," U.S. Department of Energy, Jun. 2010.
- [62] R. M. Houston and G. Domahidy, "Steam Stripping: A New Process for Control of H₂S Emissions from Geothermal Power Plants," *Geotherm. Resour. Counc. Trans.*, vol. 5, pp. 471–474, Oct. 1981.
- [63] D. Gallup, "'BIOX' - A New Hydrogen Sulfide Abatement Technology for the Geothermal Industry," *Geotherm. Resour. Counc. Trans.*, vol. 16, pp. 591–596, Oct. 1992.
- [64] D. Gallup, "'BIOX' Hydrogen Sulfide Abatement Process," *Geotherm. Resour. Counc. Trans.*, vol. 20, pp. 11–17, Oct. 1996.
- [65] California Regional Water Quality Control Board - Colorado River Basin Region, "Water Discharge Requirements for Hudson Ranch Power I LLC," R7-2013-0059, Jun. 2013.

- [66] Environmental Management Associates, “Hudson Ranch II Geothermal Project Imperial County, California. Operational Processes and Air Pollutant Emissions,” EnergySource LLC, 2135-04, Apr. 2012.
- [67] E. Gunnlaugsson and G. Gislason, “Preparation for a new power plant in the Hengill geothermal area, Iceland,” in *Proceedings World Geothermal Congress 2005, Antalya, Turkey*, 2005.
- [68] Mannvit Engineering, “Hellisheidi Geothermal Power Plant, Iceland.” [Online]. Available: <http://www.mannvit.com/GeothermalEnergy/ProjectExampleinfo/hellisheidi-geothermal-power-plant>. [Accessed: 26-Oct-2013].
- [69] A. Ragnarsson, “Utilization of geothermal energy in Iceland,” in *Proceedings of the International Geothermal Conference IGC-2003*, 2003, pp. 39–45.
- [70] Orkustofnun, “Greenhouses | National Energy Authority of Iceland,” *Geothermal - Direct Utilization*, Jun-2013. [Online]. Available: <http://www.nea.is/geothermal/direct-utilization/greenhouses/>. [Accessed: 07-Jun-2013].
- [71] J. M. Smith, H. C. Van Ness, and M. M. Abbott, *Introducción a la termodinámica en ingeniería química*. México [etc.]: McGraw-Hill, 2007.
- [72] J. A. Bierlein and W. B. Kay, “Phase-Equilibrium Properties of System Carbon Dioxide-Hydrogen Sulfide,” *Ind. Eng. Chem.*, vol. 45, no. 3, pp. 618–624, Mar. 1953.
- [73] Chemical Engineering and Materials Research Information Center, “Binary Vapor-Liquid Equi. Data.” [Online]. Available: <http://www.thermo.com/research/kdb/hcvle/showvle.php?vleid=335>. [Accessed: 02-Nov-2013].
- [74] *Perry’s chemical engineers’ handbook*, 8th ed. New York: McGraw-Hill, 2008.
- [75] H. Z. Kister, *Distillation design*. New York: McGraw-Hill, 1992.
- [76] W. L. McCabe, J. C. Smith, and P. Harriott, *Operaciones unitarias en ingeniería química*. Madrid: McGraw-Hill, 1994.
- [77] B. Roffel, B. H. L. Betlem, and J. A. F. de Ruijter, “First principles dynamic modeling and multivariable control of a cryogenic distillation process,” *Comput. Chem. Eng.*, vol. 24, no. 1, pp. 111–123, Apr. 2000.

- [78] T. M. Flynn, *Cryogenic engineering*, 2nd ed., rev. and expanded. New York: Marcel Dekker, 2005.
- [79] M. I. Khan, *The petroleum engineering handbook: sustainable operations*. Houston, TX: Gulf Pub, 2007.
- [80] S. Gao, W. House, and W. G. Chapman, "NMR/MRI study of clathrate hydrate mechanisms," *J. Phys. Chem. B*, vol. 109, no. 41, pp. 19090–19093, 2005.
- [81] S. Gao, W. G. Chapman, and W. House, "NMR and Viscosity Investigation of Clathrate Hydrate Formation and Dissociation," *Ind. Eng. Chem. Res.*, vol. 44, no. 19, pp. 7373–7379, Sep. 2005.
- [82] O. Urdahl, B. J. R. Atle, K. Kinnari, and R. Holme, "Operational experience by applying direct electrical heating for hydrate prevention," in *Offshore Technology Conference*, 2003.
- [83] Z. Huo, E. Freer, M. Lamar, B. Sannigrahi, D. J. Knauss, and E. D. Sloan Jr., "Hydrate plug prevention by anti-agglomeration," *Chem. Eng. Sci.*, vol. 56, no. 17, pp. 4979–4991, Sep. 2001.
- [84] J. P. Lederhos, J. P. Long, A. Sum, R. L. Christiansen, and E. D. Sloan Jr., "Effective kinetic inhibitors for natural gas hydrates," *Chem. Eng. Sci.*, vol. 51, no. 8, pp. 1221–1229, Apr. 1996.
- [85] C. A. Koh, R. E. Westacott, W. Zhang, K. Hirachand, J. L. Creek, and A. K. Soper, "Mechanisms of gas hydrate formation and inhibition," *Fluid Phase Equilibria*, vol. 194–197, pp. 143–151, Mar. 2002.
- [86] M. A. Kelland, T. M. Svartås, and L. D. Andersen, "Gas hydrate anti-agglomerant properties of polypropoxylates and some other demulsifiers," *J. Pet. Sci. Eng.*, vol. 64, no. 1–4, pp. 1–10, Feb. 2009.
- [87] E. W. Lemmon, M. O. McLinden, and D. G. Friend, *NIST Chemistry WebBook, NIST Standard Reference Database Number 69*. Gaithersburg, MD.: P.J. Linstrom and W.G. Mallard, National Institute of Standards and Technology.

9. Appendices

A. Properties of CO₂ and H₂S

Table 22: Thermophysical properties of CO₂ at 4MPa

Temperature (C)	Density (kg/m ³)	Volume (m ³ /kg)	Enthalpy (kJ/mol)	Cv (J/mol*K)	Cp (J/mol*K)
-50	1162.2	8.60E-04	4.1266	42.667	85.639
-45	1143.8	8.74E-04	4.5564	42.365	86.293
-40	1124.8	8.89E-04	4.9898	42.081	87.123
-35	1105.1	9.05E-04	5.4279	41.818	88.163
-30	1084.6	9.22E-04	5.8719	41.576	89.455
-25	1063.2	9.41E-04	6.323	41.36	91.064
-20	1040.7	9.61E-04	6.7832	41.177	93.078
-15	1016.8	9.84E-04	7.2547	41.046	95.635
-10	991.09	1.01E-03	7.7408	41.002	98.954
-5	963.16	1.04E-03	8.2461	41.097	103.42
0	932.11	1.07E-03	8.7781	41.403	109.8
5	896.39	1.12E-03	9.35	42.043	119.8
5.2997	894.05	1.12E-03	9.386	42.097	120.59
5.2997	115.74	8.64E-03	18.803	40.079	95.247
10	108.41	9.22E-03	19.213	37.921	80.624
15	102.39	9.77E-03	19.592	36.528	71.814
20	97.492	1.03E-02	19.936	35.604	66.131
25	93.349	1.07E-02	20.256	34.961	62.145
30	89.759	1.11E-02	20.559	34.5	59.194

Table 23: Thermophysical properties of H2S at 4MPa

Temperature (C)	Density (kg/m3)	Volume (m3/kg)	Enthalpy (kJ/mol)	Cv (J/mol*K)	Cp (J/mol*K)
-80	986.21	1.01E-03	-1.25	43.84	68.33
-75	977.85	1.02E-03	-0.91	43.30	68.09
-70	969.42	1.03E-03	-0.57	42.79	67.91
-65	960.92	1.04E-03	-0.23	42.31	67.76
-60	952.34	1.05E-03	0.11	41.85	67.67
-55	943.66	1.06E-03	0.44	41.41	67.62
-50	934.88	1.07E-03	0.78	40.99	67.61
-45	925.99	1.08E-03	1.12	40.60	67.65
-40	916.97	1.09E-03	1.46	40.22	67.73
-35	907.82	1.10E-03	1.80	39.87	67.87
-30	898.53	1.11E-03	2.14	39.53	68.05
-25	889.07	1.12E-03	2.48	39.20	68.30
-20	879.43	1.14E-03	2.82	38.90	68.59
-15	869.6	1.15E-03	3.16	38.60	68.95
-10	859.56	1.16E-03	3.51	38.33	69.38
-5	849.28	1.18E-03	3.86	38.07	69.88
0	838.74	1.19E-03	4.21	37.82	70.47
5	827.91	1.21E-03	4.56	37.59	71.15
10	816.75	1.22E-03	4.92	37.37	71.94
15	805.23	1.24E-03	5.28	37.16	72.86
20	793.3	1.26E-03	5.65	36.97	73.93
25	780.9	1.28E-03	6.02	36.80	75.18
30	767.95	1.30E-03	6.40	36.64	76.66

Table 24: Thermophysical properties of CO2 at 2MPa

Temperature (C)	Density (kg/m3)	Volume (m3/kg)	Enthalpy (kJ/mol)	Cv (J/mol*K)	Cp (J/mol*K)
-50	1157.6	8.64E-04	4.0283	4.1043	25.336
-45	1138.8	8.78E-04	4.4603	4.5376	27.257
-40	1119.3	8.93E-04	4.8966	4.9753	29.154
-35	1099	9.10E-04	5.3383	5.4184	31.035
-30	1077.8	9.28E-04	5.7868	5.8685	32.905
-25	1055.5	9.47E-04	6.2438	6.3272	34.772
-20	1031.8	9.69E-04	6.7117	6.7970	36.646
-19.503	1029.4	9.71E-04	6.7589	6.8444	36.834
-19.503	52.54	1.90E-02	17.5500	19.2260	85.647
-15	50.632	1.98E-02	17.7380	19.4760	86.626
-10	48.765	2.05E-02	17.9370	19.7420	87.645
-5	47.104	2.12E-02	18.1280	19.9970	88.606
0	45.608	2.19E-02	18.3140	20.2440	89.519
5	44.246	2.26E-02	18.4960	20.4850	90.394
10	42.997	2.33E-02	18.6750	20.7220	91.236
15	41.844	2.39E-02	18.8500	20.9540	92.049
20	40.773	2.45E-02	19.0240	21.1830	92.837
25	39.773	2.51E-02	19.1960	21.4090	93.603
30	38.837	2.57E-02	19.3670	21.6340	94.349

Table 25: Thermophysical properties of H2S at 2MPa

Temperature (C)	Density (kg/m3)	Volume (m3/kg)	Enthalpy (kJ/mol)	Cv (J/mol*K)	Cp (J/mol*K)
-80	984.67	1.02E-03	-1.3694	-1.3002	-6.740
-75	976.23	1.02E-03	-1.0284	-0.9586	-4.994
-70	967.73	1.03E-03	-0.6884	-0.6180	-3.296
-65	959.15	1.04E-03	-0.3492	-0.2781	-1.643
-60	950.47	1.05E-03	-0.0105	0.0612	-0.032
-55	941.7	1.06E-03	0.3279	0.4003	1.540
-50	932.82	1.07E-03	0.6662	0.7393	3.076
-45	923.82	1.08E-03	1.0046	1.0784	4.579
-40	914.68	1.09E-03	1.3435	1.4180	6.052
-35	905.4	1.10E-03	1.6830	1.7583	7.496
-30	895.96	1.12E-03	2.0234	2.0995	8.914
-25	886.35	1.13E-03	2.3650	2.4419	10.308
-20	876.54	1.14E-03	2.7082	2.7859	11.680
-15	866.53	1.15E-03	3.0531	3.1318	13.033
-10	856.28	1.17E-03	3.4002	3.4798	14.368
-5	845.76	1.18E-03	3.7499	3.8305	15.689
0	834.96	1.20E-03	4.1027	4.1843	16.996
5	823.84	1.21E-03	4.4589	4.5417	18.292
10	812.35	1.23E-03	4.8193	4.9032	19.580
15	800.45	1.25E-03	5.1845	5.2696	20.863
20	788.07	1.27E-03	5.5553	5.6418	22.144
24.648	776.07	1.29E-03	5.9061	5.9939	23.335
24.648	33.594	2.98E-02	18.1600	20.1890	71.002
25	33.519	2.98E-02	18.1730	20.2070	71.061
30	32.502	3.08E-02	18.3540	20.4510	71.874

B. Physical correlations employed

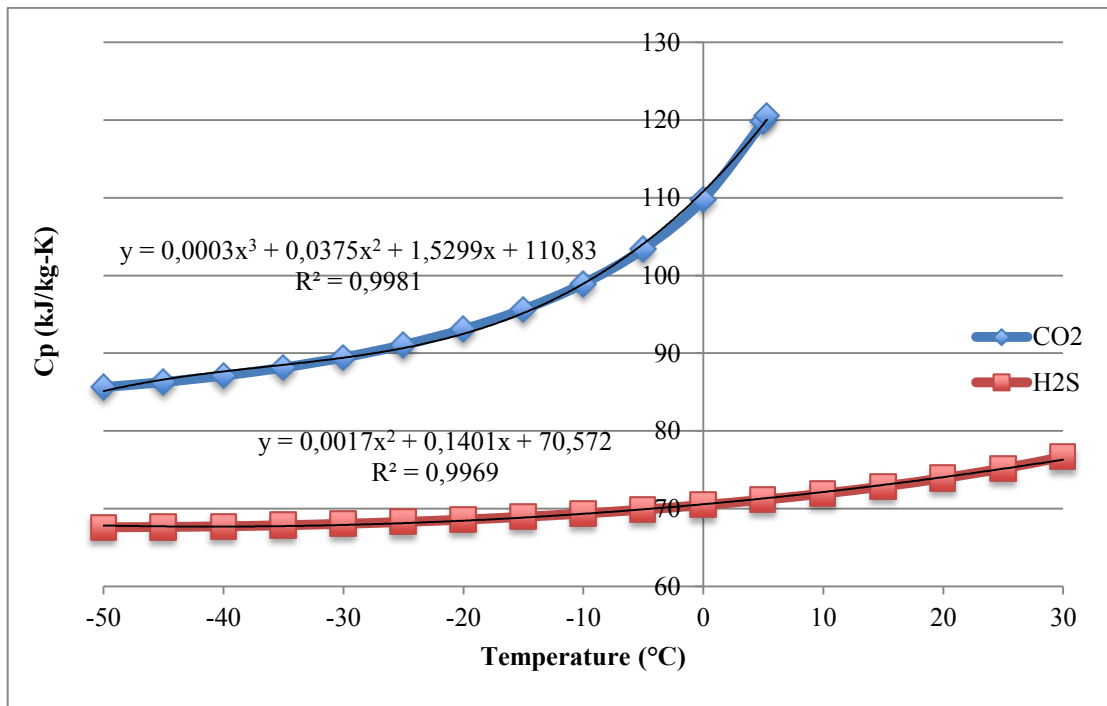


Figure 11: Correlation employed for calculation of Specific Heat at constant pressure of CO₂ and H₂S, 4MPa

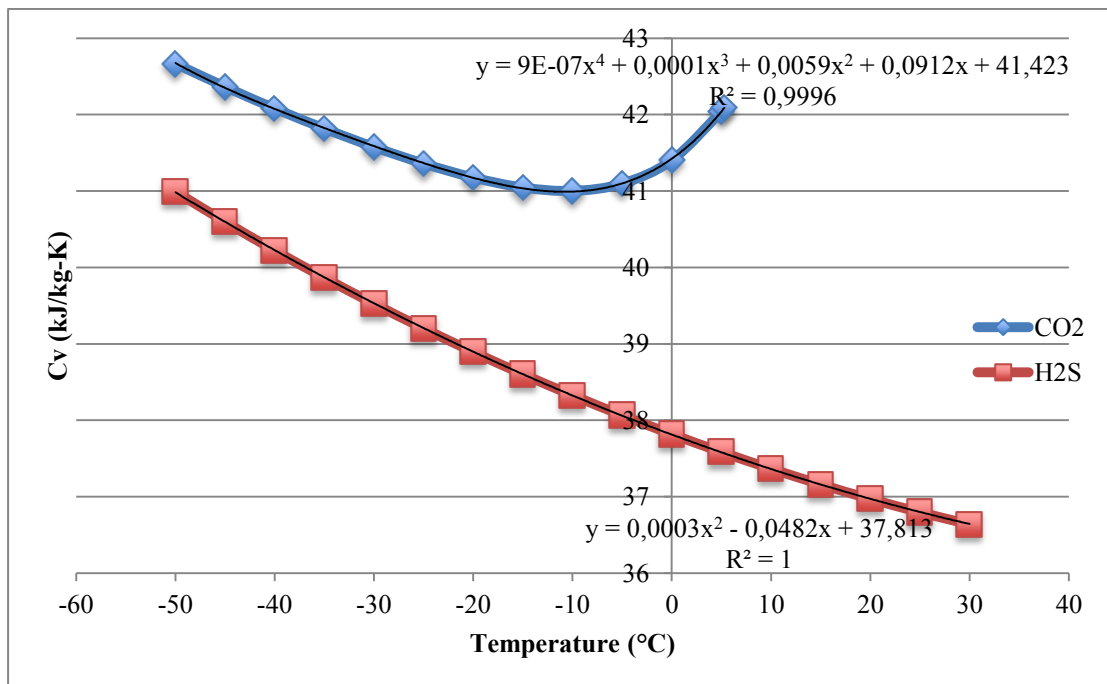


Figure 12: Correlation employed for the calculation of Specific Heat at constant volume of CO₂ and H₂S, 4MPa

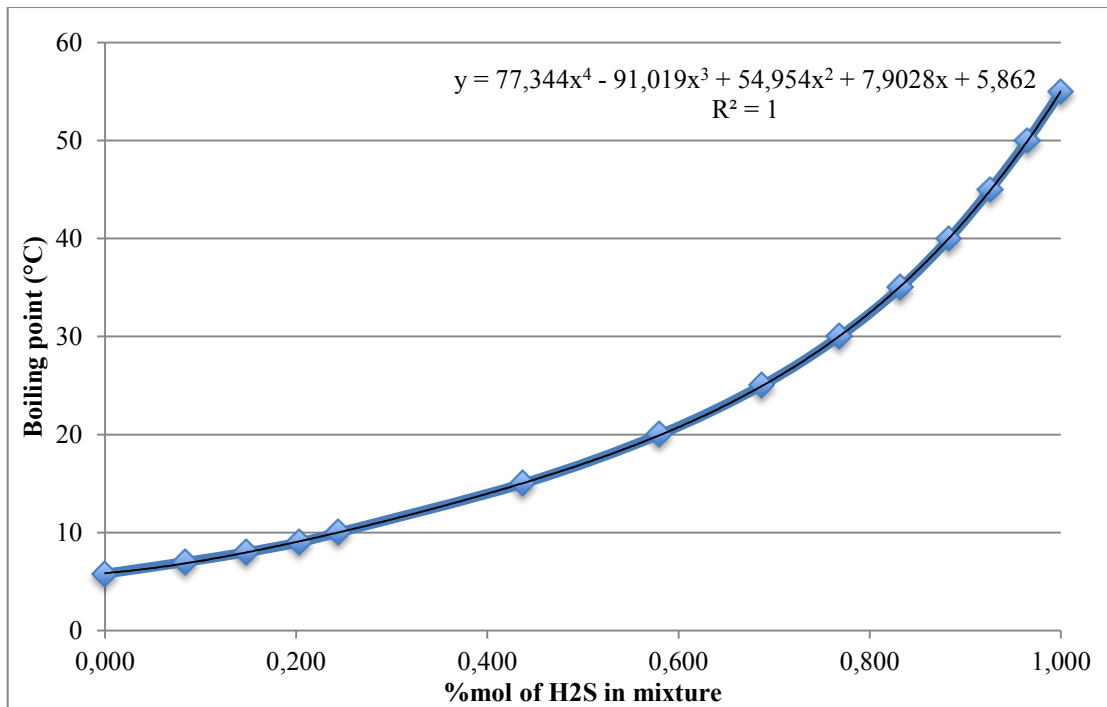


Figure 13: Correlation used for calculation of mixture boiling point 4MPa

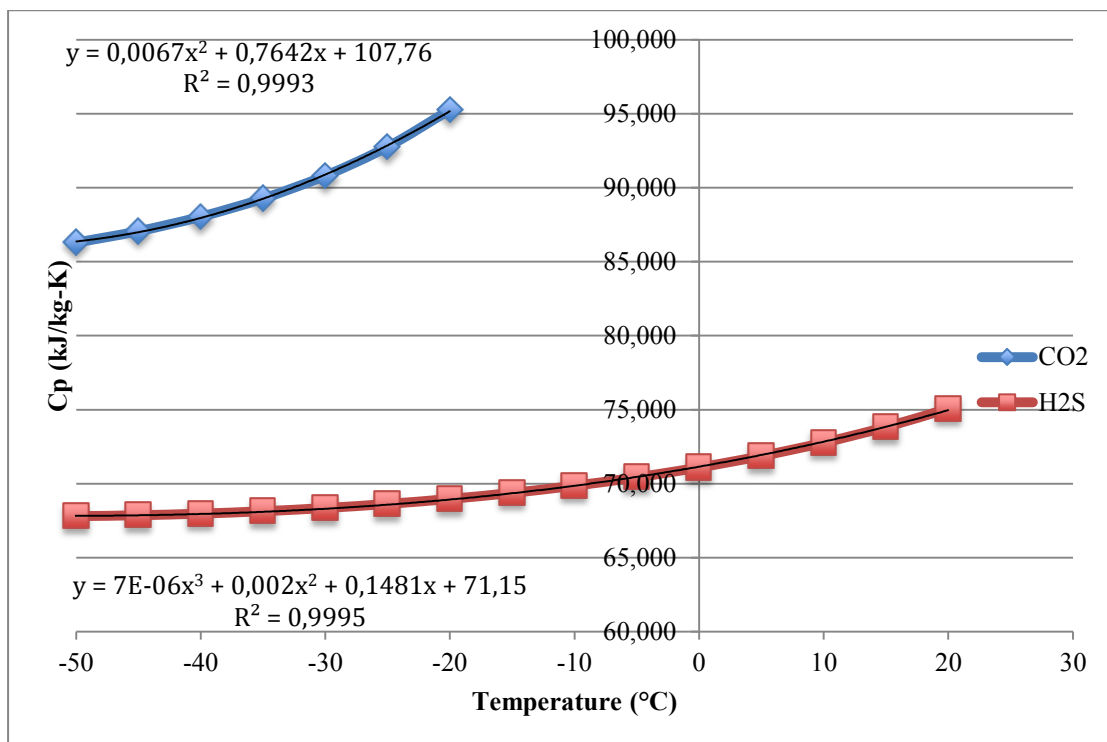


Figure 14: Correlation used for calculation of heat capacity at constant pressure, 2MPa

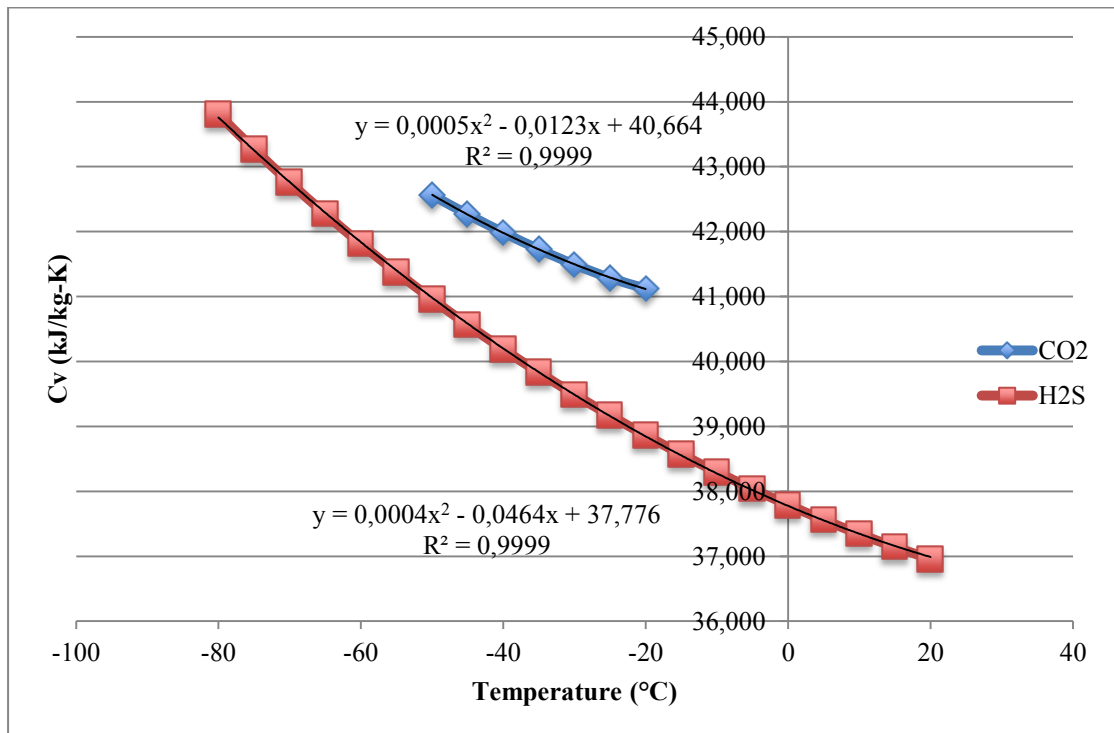


Figure 15: Correlation used for calculation of heat capacity at constant volume, 2MPa

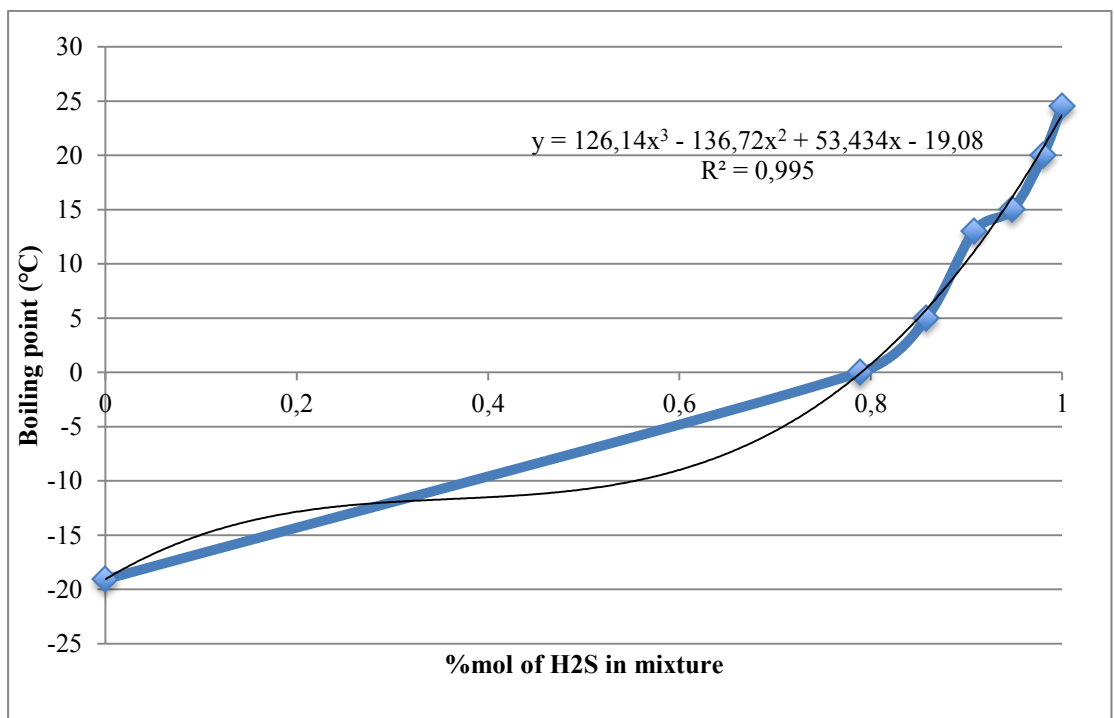


Figure 16: Correlation used for calculation of boiling point of mixture, 2MPa

C. McCabe Thiele Diagram

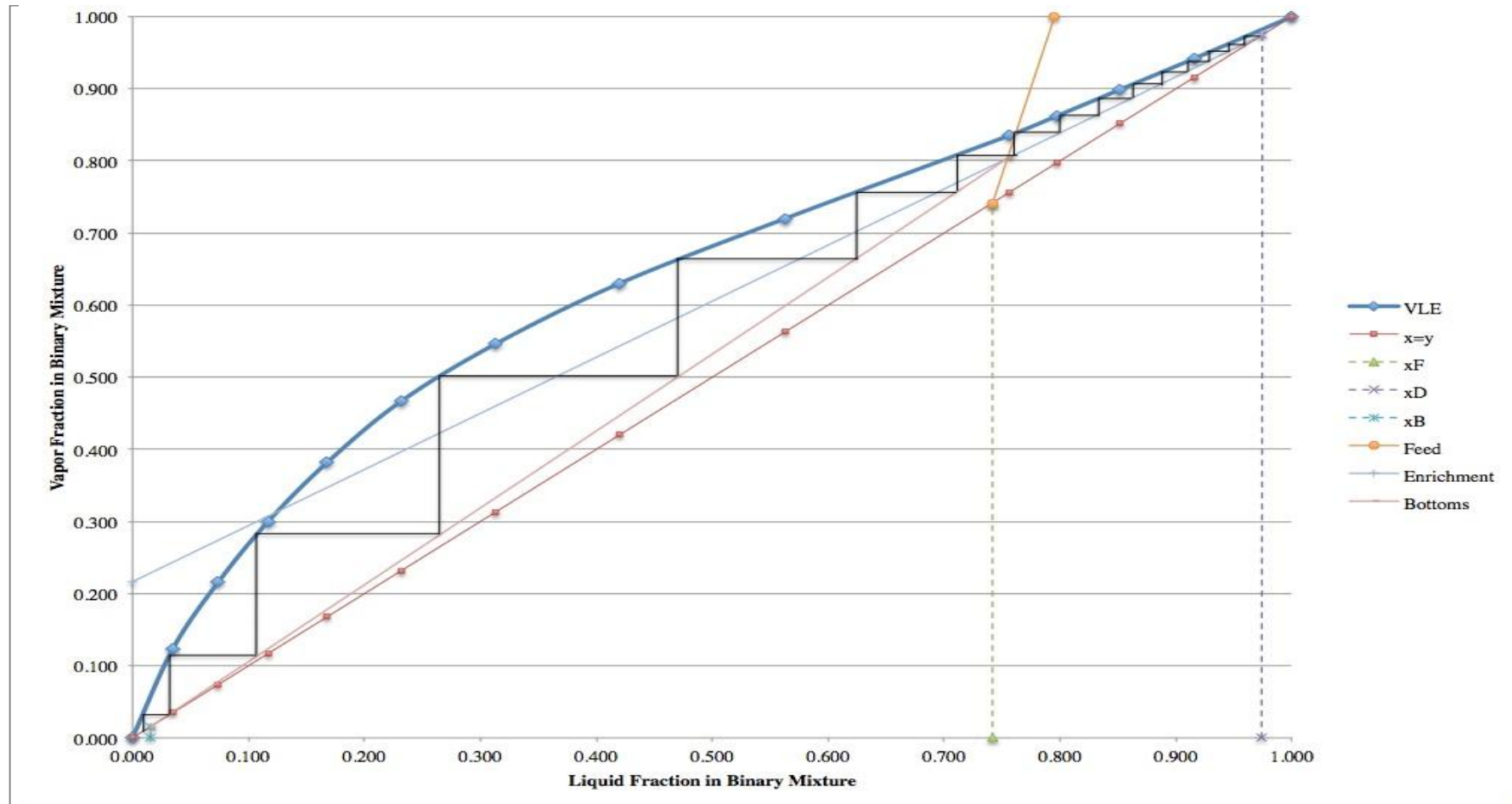


Figure 17: McCabe Thiele Diagram of distillation process at 40bar

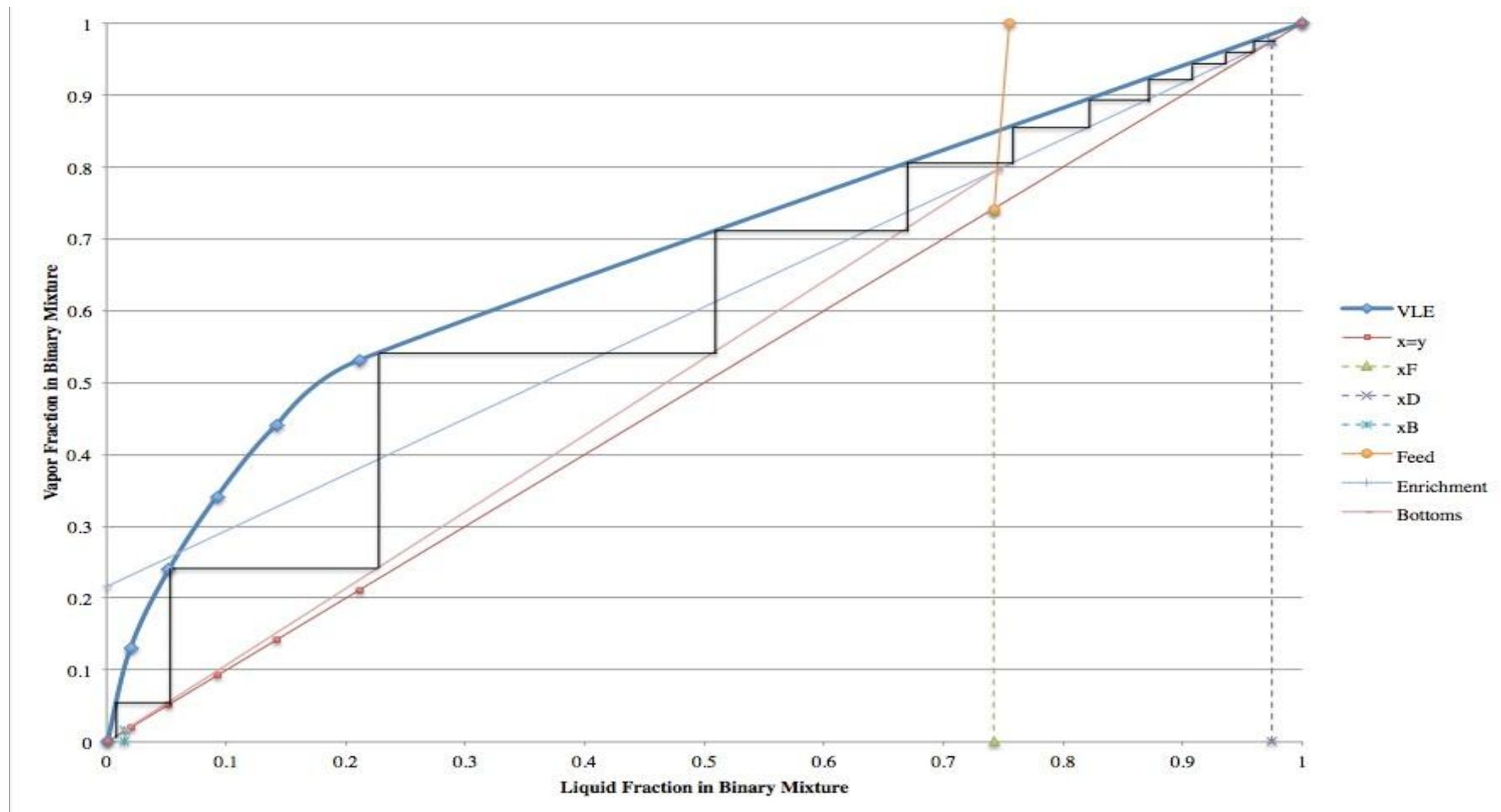


Figure 18: McCabe-Thiele Diagram of distillation process at 20bar

D. Column diameter

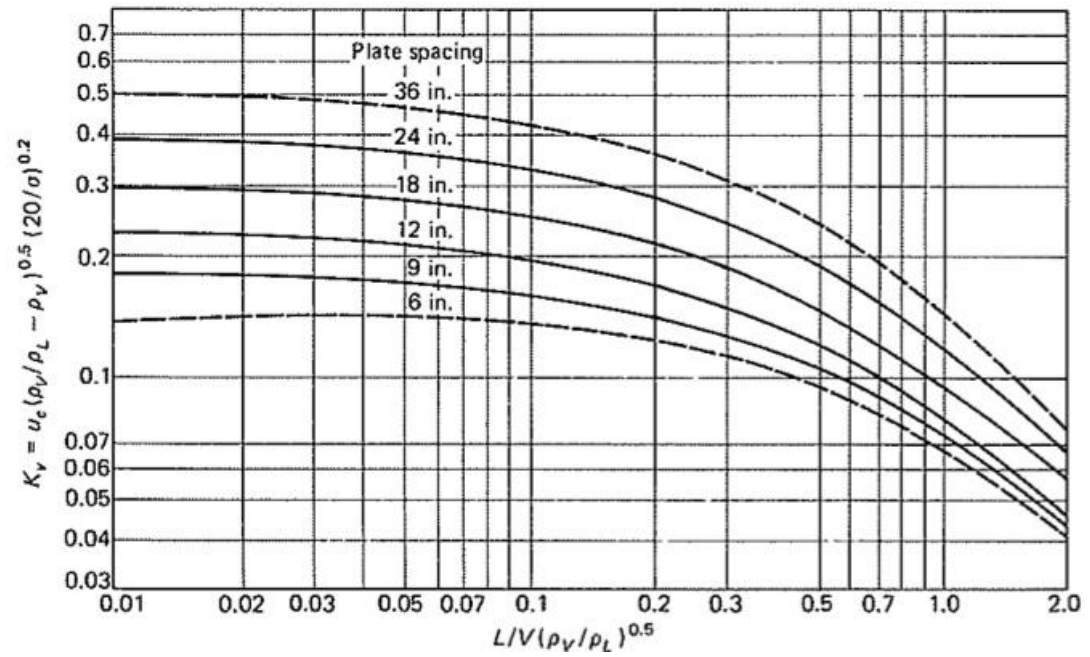


Figure 19: Kv values for perforated plates under flooding conditions